Title: Evidence of low watershed resilience across the Western United States

Authors: Nicholas E. Kolarik *[a], Alex Brooks [b], T. Trevor Caughlin [c], Eric Jensen [b], Louis Jochems [d], Jodi Brandt [a]

[a] Human Environment Systems, Boise State University, 1910 University Drive, Boise, ID 83275.
[b] Desert Research Institute, 2215 Raggio Parkway Reno, NV 89512.
[c] Department of Biological Sciences, Boise State University, 1910 University Drive, Boise, ID 83275.
[d] Trout Unlimited, 910 W Main St #342, Boise, ID 83702

Abstract

Vulnerable waters, including headwater streams and non-floodplain wetlands, are essential to watershed level resilience but notoriously difficult to measure over large spatial scales. Although individually small, vulnerable waters as a whole are integral in regulating hydrologic and biogeochemical processes. In the relatively small proportion of vulnerable waters that are continuously monitored, there are clear signs of declining water availability and resilience. However, the dispersed and remote nature of these waters makes continuous, landscape-scale monitoring impossible with traditional in situ methods, limiting our understanding of their condition. To address this gap, we produced a satellite-derived dataset of monthly ecologically-available water in vulnerable waters during the growing season from 2016 to 2024 across dryland ecoregions in the western United States. We then developed several indicators of conditions in vulnerable waters. Our results uncover varying levels of degradation in headwaters across the western U.S., and indicate that many watersheds may have very low resilience to climate or land-use shocks. In these watersheds, the functions provided by vulnerable waters, such as maintaining flow heterogeneity, sediment connectivity, water availability, and habitat heterogeneity, may be declining and threatened. We demonstrate the utility of the dataset we introduce in this study for identifying watersheds where functions have become limited and could be good targets for restoration efforts. Overall, we demonstrate that satellite-based measurements fill a major monitoring gap for vulnerable waters, and these continuous time-series measures across entire landscapes have the potential to transform our understanding of how vulnerable waters are changing over time. The metrics we calculated from the pixel-based maps are able to summarize important ecosystem function characteristics, and can be used to answer a variety of scientific questions and inform management decisions. Furthermore, our approach is completely open access and reproducible for future years and in other dryland biomes.

Keywords: remote sensing, resilience, watersheds, wetlands, watershed management, headwaters

1. Introduction

Anthropogenic changes to Earth Systems threaten the functioning and maintenance of life on Earth (Rockström et al., 2023). Changes in the global water cycle exacerbate these changes, the impacts of which will reach all corners of the globe to varying extents (Allan et al., 2020). Altered timing and quantity of precipitation inputs and shifts from snow to rain trigger changes that reverberate throughout ecosystems (Hale et al., 2023; Pilliod et al., 2022; Uzun et al., 2021). Land cover changes decrease groundwater storage and contributions to base flows, increased vapor deficits increase wildfire risk, and higher temperatures affect vegetation, wildlife, and evaporative demands for crops (Abatzoglou and Williams, 2016; Brooks et al., 2025; Donnelly et al., 2020). While researchers before us have studied some effects of an altered water cycle, many effects remain highly uncertain (Gleick, 2010).

Water limited regions, hereafter drylands, cover 40% of the Earth's surface and are home to about a third of the human population (Prăvălie, 2016). The health and functions of these ecoregions hinge on headwater streams and isolated, non-floodplain wetlands (hereafter referred to as *vulnerable waters*) and the processes they support (Lane et al., 2023; Poff et al., 2012). While vulnerable waters account for a very small portion of the landscape, they host the majority of ecologically available water (i.e. surface water and shallow groundwater) in dryland regions. Vulnerable waters are increasingly displaced, confined, and altered for agriculture and development despite being disproportionately important for maintaining biodiversity and landscape level functions (Ahmed and Jackson-Smith, 2019; Macfarlane et al., 2017a; Maestas et al., 2001). Increasing aridification, growing populations, and associated land cover changes exacerbate this issue and monitoring these small, but important ecosystems has never been more relevant (Belote et al., 2021; Gleick, 2010).

Vulnerable waters contribute to, and are indicative of, watershed health and resilience (Lane et al., 2023). Though relatively small as individual units, they aggregate to cumulatively immense impacts on watershed processes (Christensen et al., 2022). Human and wildlife populations are dependent on hydrological processes, including surface and shallow ground water flow regulation, determined by the spatial arrangement of these dispersed but ubiquitous landscape features (Donnelly et al., 2016; Evenson et al., 2018a; Fremier et al., 2015; Mushet et al., 2019). Further, vulnerable waters regulate biogeochemical flows, including carbon sequestration, essential to mitigating greenhouse gas emissions and achieving carbon neutrality (Hu et al., 2022; Lane et al., 2025; Marton et al., 2015), and are instrumental in regulating sediment regimes and transport often interrupted by anthropogenic land cover changes (Beechie et al., 2010; Wohl et al., 2024). However impactful, the functions of vulnerable waters are notoriously difficult to monitor across large areas due to their small size, remote and sometimes poorly mapped locations, and the amount of time and resources needed to effectively measure each of the aforementioned phenomena *in situ* (Castellazzi et al., 2019; Creed et al., 2017).

Functions in vulnerable waters are becoming increasingly limited due to land cover conversions and variable precipitation inputs and timing (Evenson et al., 2018a). Shifts from mesic towards xeric vegetation types indicate a lack of ecologically available water and a reliance on precipitation rather than near-surface groundwater maintained by intact systems (Pollock et al., 2014; Wohl, 2021). Land managers across dryland regions in the western U.S. are actively trying to reverse these shifts, typically seeking to reduce the reliance on precipitation inputs for ecologically available water by restoring the geomorphological processes that foster hydrologic connectivity (Beechie et al., 2010; Pollock et al., 2014; Silverman et al., 2019). By doing so, they seek to increase the stability of these keystone landscape features, decrease the flashiness, or variability that affects the watershed-scale contributions to steady-state dynamics (Cartwright and Johnson, 2018). With insufficient monitoring tools, however, there is a substantial gap in our understanding of the changes in functions delivered via the hydrological cycle that occur in vulnerable waters.

Variability has been demonstrated to be a good measure of system stability, and flashiness of hydrologic systems specifically (Dakos and Kéfi, 2022; Vanderhoof et al., 2025). Identifying systems that are becoming flashier, and thus more variable, could help to prioritize locations where the functions of vulnerable waters are threatened for interventions. However, researchers have highlighted the lack of developed spatial data available and discuss their inability to effectively monitor the dynamics of vulnerable waters across large spatial scales (Christensen et al., 2022). The disparate datasets available are currently unable to map their spatial extent, configuration, temporal fluxes and interactions, thresholds and drivers of change, and use technical advances such as big data to understand the scale of influence (Lane et al., 2023). Regional level objectives for vulnerable waters are difficult to establish due to disparate datasets, overlapping jurisdictions, and inadequate in situ monitoring (Gleick, 2010). As a result, policy objectives and water programs are currently at a loss for communicating outcomes of any efforts taken.

Here, we provide unprecedented spatial and temporal details about the state and dynamics of vulnerable waters across drylands in the western U.S. We developed satellite-based time-series from freely available satellite imagery, machine learning, and cloud computing. The dataset we present contains monthly measures of vulnerable waters' condition at 10m spatial resolution during the growing season across the entire landscape from 2016 to 2024. We then summarized these time-series into indicators of intactness (proportion of vulnerable waters area occupied with mesic vegetation, see Methods), variability (i.e. flashiness) indicative of a lack of resilience, and association of water availability with climate. We provide summaries of these metrics at the subwatershed and ecoregion scales. Finally, we discuss spatial and temporal patterns of vulnerable waters across our broad study area, their implications for policy, and how these measures can provide insights to many of the *needs informing the maintenance of watershed resilience* (Lane et al., 2023).

2. Methods

2.1 Study area

The sagebrush biome is a dryland region of the western United States that occupies at least some of all states entirely west of the 100th meridian, and some in the northern Great Plains region (Figure 1). While this region is one of the world's least developed, it faces many complex pressures and is considered to be one of the most threatened in the country (Doherty et al., 2024). Though the entire region is considered water-limited, and the mean annual precipitation is ~398 mm (rain and melted snow), there is considerable variation throughout the region. Some areas experience less than 185 mm of annual precipitation while others receive more than 807 mm (5% of the study area, respectively) (Daly and Bryant, 2013). Land managers in the sagebrush biome have shifted focus in recent years from wildlife species-specific management towards threat-based ecosystem management, requiring restoration and conservation targeting at greater spatial scales (Doherty et al., 2022; Mozelewski et al., 2024). Although many of the threats that are routinely discussed focus on upland ecosystems (e.g. annual invasive grasses,

conifer encroachment (Maestas et al., 2022; Reinhardt et al., 2020)), there have been specific calls to better understand mesic ecosystems that this ecoregion relies upon for water resources and associated habitats (Doherty et al., 2024).

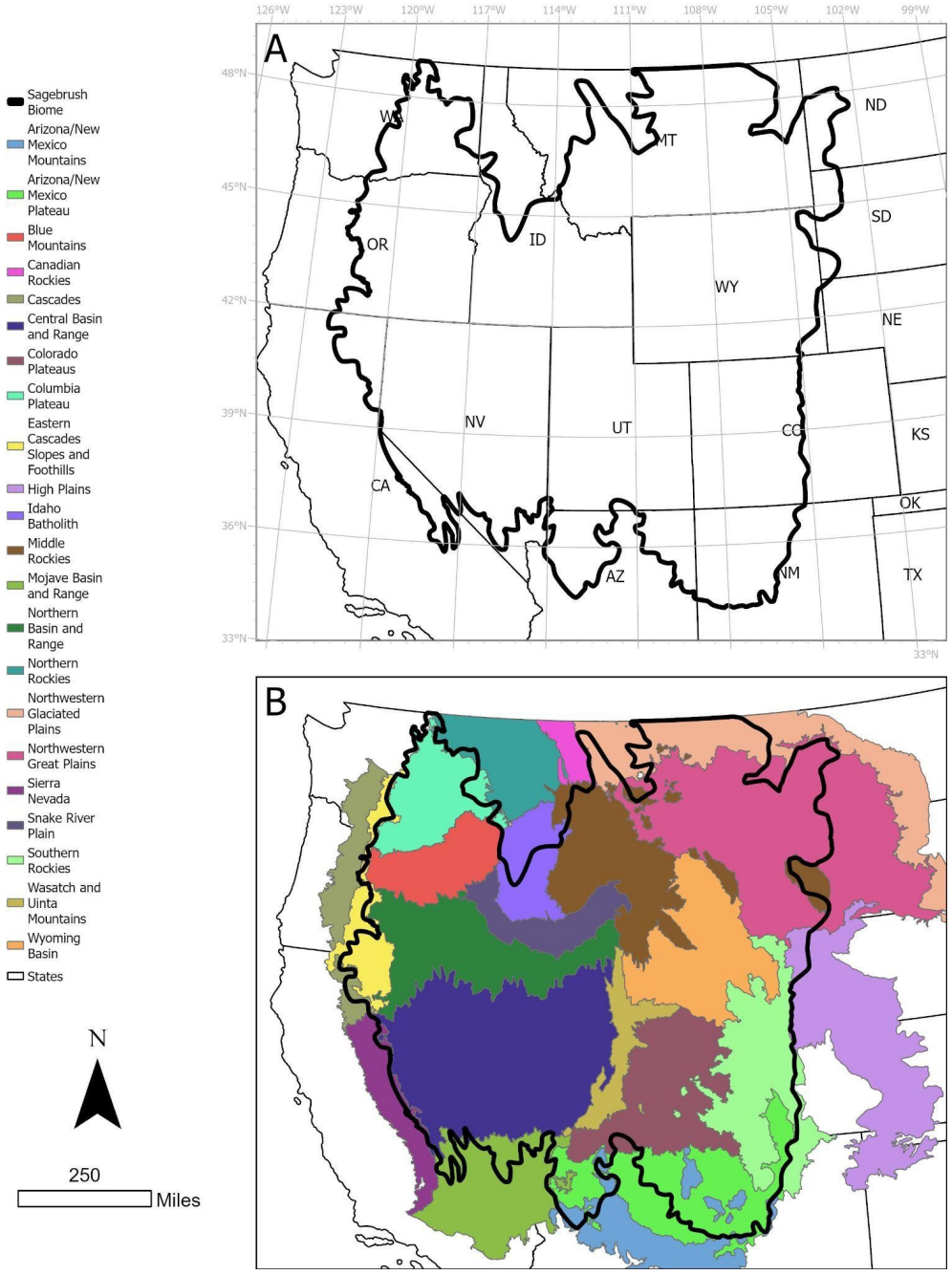

Figure. 1. A) Location of the sagebrush biome relative to the Western United States and B) EPA level III ecoregions.

2.2 Data

2.2.1 Satellite imagery

The classified maps we produced are based on the Sentinel time series. Due to varying gaps in available Sentinel-2 and Sentinel-1 data across space and time, we parameterized identical models with varying underlying input images to ensure complete map coverage (Figure S1). For the years of 2016 through 2018 we used the Sentinel-2 level 1C top of atmosphere (TOA) harmonized collection and the Sentinel-1 C-band Synthetic Aperture Radar (SAR) Ground Range Detected (GRD) images from ascending paths (data gaps for descending paths). Though the time series of level-2A surface reflectance images during these years had substantial data gaps, TOA images have been shown to satisfactorily separate land cover classes such as surface water, mesic, and upland vegetation (Kolarik et al., 2023; Pickens et al., 2020). From 2019 through 2021, we parameterized a second model and used harmonized Sentinel-2 level-2A surface reflectance (SR) images along with ascending paths from the Sentinel-1 GRD time series. Finally, for the model from 2022 through 2024, we again used the harmonized Sentinel-2 level 2A SR images, but with descending paths from the Sentinel-1 GRD data. We are relegated to the use of descending paths due to an anomalous failure of the power supply electronics that led to the end of the mission for the Sentinel-1B satellite (European Space Agency, 2022).

For all models, we filtered the collection to remove images with greater than 50% clouds resulting in 119,459 images (30,968, 42,872, 45,619 images respectively). We then masked clouds from each image using the *s2cloudless* dataset (Zupanc, 2020). With these cloud-masked image collections, we prepared image stacks for classification using all visible, near-infrared (NIR), and shortwave infrared (SWIR) bands available in the Sentinel-2 images (Table 1). We used these bands to calculate commonly used normalized difference indices for vegetation and water to help distinguish between land cover classes, which we added to the stack. We created bands to indicate latitude and longitude of each pixel to control for effects of spatial autocorrelation throughout the study region. We then masked known areas of lava flows and built environment, which are a known source of confusion for water classifications (European Commission, 2023; Pekel et al., 2016).

Regardless of the path of the available Sentinel-1 data, we created annual means of the backscatter measurements of the GRD images. We did this as both a space for time substitution to reduce the inherent speckle in the SAR images, as well as to deal with the varying data gaps throughout the time series. While researchers commonly use a spatial filter for decreasing speckle in backscatter images, this risks underestimating the extents of classes of interest near their boundaries and could result in small wetted areas being omitted entirely (Behnamian et al., 2017). We filtered the SAR collection for images from May through October and created mean composites for both VV and VH polarizations, known to be effective for identifying differences in soil moisture and vegetation density, respectively (Kornelsen and Coulibaly, 2013; Patel et al., 2006). We considered growing season composites to be sufficient, given vegetation structure within this period at the 10-m scale should remain relatively constant.

Table 1. Covariates used in classification

Layer	Source	GSD
Blue	Sentinel-2 (B2)	10 m
Green	Sentinel-2 (B3)	10 m
Red	Sentinel-2 (B4)	10 m
Red edge	Sentinel-2 (B5)	20 m
Red edge	Sentinel-2 (B6)	20 m
Red edge	Sentinel-2 (B7)	20 m
Near-infrared	Sentinel-2 (B8)	10 m
Near-infrared	Sentinel-2 (B8A)	20 m
Short-wave infrared	Sentinel-2 (B11)	20 m
Short-wave infrared	Sentinel-2 (B12)	20 m
Latitude	Sentinel-2	10 m
Longitude	Sentinel-2	10 m
re1NDVI	Sentinel-2	20 m
re2NDVI	Sentinel-2	20 m
re3NDVI	Sentinel-2	20 m
NDVI	Sentinel-2	10 m
Narrow-band NDVI	Sentinel-2	20 m
NDWI	Sentinel-2	10 m
MNDWI	Sentinel-2	20 m
VV	Sentinel-1	10 m
VH	Sentinel-1	10 m
TWI	SRTM	30 m
Slope	NED	10 m
Aspect	NED	10 m
Wetland probability	Landsat/SRTM	30 m

2.2.2 Ancillary variables

Beyond the satellite images we included topographic layers that determine hydrological processes, and thus likelihood of ecologically available water. In each image stack we included a 30 m topographic wetness index (TWI) developed by (Hoylman, 2021) from the Shuttle Radar Topography Mission (SRTM) and terrain metrics (slope and aspect maps) which we produced

from the 10 m National Elevation Dataset (NED) and are determinants of soil moisture (Western et al., 1999). We included a wetland probability layer produced using both Landsat metrics and hydrologic metrics from the SRTM (Bwangoy et al., 2010; Hansen et al., 2021; Margono et al., 2014), along with the latitude and longitude of each pixel. Each of these help the classifier differentiate between any spectrally similar classes that occur in varying topographical contexts.

2.3 Classification

2.3.1 Training data

After filtering and masking the image collection, we stacked each image with the ancillary covariates in preparation for classification. We began by collecting samples from at least 20 randomly sampled Sentinel-2 images throughout the spatial and temporal domains for each model. We sampled instances of surface water, mesic vegetation, upland areas, snow, and shadows in images from May to October to sufficiently capture any extreme conditions we might encounter during the growing season classifications. If we noticed any biases in initial outputs (differences in spatial performance, errors associated with specific land covers), we iteratively added instances of problematic classes from additional randomly sampled images to improve representation in the training set. This process resulted in a sample pool of over 16 million pixels to capture the range of variability in our study area.

2.3.2 Validation data

We used a probabilistic sampling design to create an independent dataset to assess the accuracy of the maps (Pickens et al., 2020; Stehman and Foody, 2019). First, we collapsed classes for upland areas, snow, and shadow into one ‘other’ class. We did this because salt flats and snow were commonly confused, but distinguishing between them was not a focus of our study. For each model, we randomly sampled 100 pixels for each class (300/model; 900 total) (Kolarik et al., 2023). Since many pixels switch labels at some point throughout the growing season, we followed a hierarchical sampling design beginning with the most rare class to the most common (surface water, mesic vegetation, other). For example if a pixel was ever classified as water in the output for a given model, we considered it to belong to the surface water sample pool. We then took a random sample of 100 points from that sample pool, and removed the entire pool of possible water samples before continuing with mesic vegetation, and so forth. This design ensures every pixel has a non-zero probability of being sampled and therefore reduces bias in our assessment (Stehman and Foody, 2019). If pixels were still indistinguishable or clearly mixed, we labeled the nearest obvious pixel. For each month, we labeled each point based on available Sentinel images and the underlying satellite basemap in GEE for additional support in instances where land covers were unclear at the 10-m spatial resolution, resulting in 3600 total points labeled.

2.3.3 Model parameterization

We used a random forest classifier with 100 trees in the forest and five variables per split (square root of count of covariates) (Belgiu and Drăguţ, 2016). These parameters balanced minimizing errors without increasing the computational time substantially. For each model, we took stratified random samples of 40,000 points from each class of collected training data to boost the sampling rates of rare classes we sought to map (e.g. mesic vegetation and surface water) (Jin et al., 2014). We classified all 119,459 image stacks from June through September. We chose this period to avoid months where the likelihood of snow and/or clouds is high while capturing the bulk of the growing season and driest parts of the water year for our study area. We then reduced these to monthly maps using the mode of all predictions throughout each monthly time series.

2.3.4 Accuracy assessment

We used a confusion matrix and an area adjusted accuracy assessment to quantify and report the accuracy and uncertainty of mapped classes (Olofsson et al., 2014). This approach accounts for the differences in inclusion probabilities for each mapped class in the accuracy assessment, accounting for the stratified sampling design we used to boost the sample sizes of rare mapped classes (Stehman and Foody, 2019). We use this design to estimate the mapped areas of each class throughout the study area and reduce errors introduced when using ‘pixel counting’ approaches (Olofsson et al., 2013). We assessed all four mapped months in 2018, 2021, and 2024 to assess each model parameterization respectively.

2.4 Developing metrics of watershed functions

We use the resilience concept to assess watershed health and functions as they relate to vulnerable waters. Resilience, at its simplest, can be considered a measure of any system to ‘absorb change and disturbance while maintaining the same relationships between populations or state variables’ (Holling, 1973). In riparian zones and non-floodplain wetlands (NFWs) we think of well connected systems as being resilient to annual drying cycles due to their hydrologic connectivity (hyporheic exchange) and ability to maintain available water throughout (Pollock et al., 2014). In semi-arid systems like the sagebrush biome, the growing season coincides with the dry season, so precipitation inputs are limited to high elevation snowmelt from the preceding wet (winter) season. When vulnerable waters are intact and well connected, they can act as sponges, maintain high water tables, provide opportunities for plentiful exchange between surface and groundwater, and are well situated to withstand the hot, dry summer months and maintain moisture throughout. However, when vulnerable waters are degraded with atypical hydrologic connectivity (e.g., ditched, straightened, abstracted, etc.), they act as conduits for moving the snowmelt through the system, reducing infiltration opportunities, and are subject to reduced function delivery as the dry season progresses. Even degraded vulnerable water systems can be wet at the beginning of the dry season, but it is the ability of these areas to maintain moisture that also aligns with the many functions they provide (e.g. improving water quality, biogeochemical flows, maintaining variation in temperatures for microhabitats (terrestrial and aquatic, etc.) (Lane et al., 2023). It is this variability that we use as a proxy for landscape

functions, with high variability indicative of low function and moderate to low variability more reliable for the delivery of these functions. Variability alone, however, cannot describe the functioning of a given riparian zone or wetland. If only a small proportion of the floodplain or wetland depression is consistently wetted, only a small fraction of the functional potential it offers is delivered, yet the variability would be low. An assessment of how much of the potential geophysical area is occupied by wetted ecosystem can return an estimate of the functioning of vulnerable waters (Kolarik et al., 2025a). On its own this proportion only describes the current state of systems well known for being highly dynamic and should be considered in tandem with variability for a more complete understanding of how the system operates.

2.4.1 Data processing

We used the classifications derived from 119,459 images from the Sentinel-2 time series along with ancillary geospatial predictors to describe intra-annual mesic vegetation cover dynamics in vulnerable waters throughout the study area. We then used some descriptive statistics of mesic vegetation cover throughout space and time in each watershed to glean insights about watershed functions as dictated by vulnerable waters. Previous research has shown that at the 10m spatial scale surface water is very rare in headwater systems, so mesic vegetation is the best proxy for ecologically available water (Kolarik et al., 2023). We identified the locations of NFWs as produced by Lane et al (Lane et al., 2023) combined with the valley bottom classifications from the Landforms dataset derived from the NED (Theobald et al., 2015) to represent NFWs and riparian zones, respectively. To focus mainly on headwaters, we used the World Wildlife Fund HydroSHEDS dataset and removed main stems (Lehner et al., 2008). This dataset, while relatively coarse, does not vary in mapping intensity across space as do others, such as the National Hydrography Flowlines dataset (Christensen et al., 2022). We used our familiarity with the study area and locations of restoration sites managed by Trout Unlimited, a non-profit organization involved in the conservation and restoration of coldwater salmonids and their habitats, to determine a reasonable threshold for differentiating headwaters from main stems with the rationale that the goals of restoration at these sites focus on improving tributaries of watersheds rather than main stems. We determined that using the hierarchical river order classification scheme the authors lay out, those that are of an order lower than seven should be removed from our analysis. We then masked a buffered distance of 500m from these lines to remove the associated floodplains of the main stems. We also masked any irrigated agriculture adjacent to remaining tributaries by using the mode of *irrMapper* time series classifications to reduce inclusion of these land covers and focus on higher functioning mesic habitats (Ketchum et al., 2020). Finally, we aggregated the remaining valley bottoms and NFWs to hydrologic unit code subwatershed (HUC12) polygons, an often used unit of management. We then aggregated all HUC12s based on the predominant Environmental Protection Agency (EPA) level III ecoregion for description.

2.4.2 Intactness

We estimate intactness by calculating the mean mesic vegetation for each HUC12 unit throughout the times series and the resilience using the coefficient of variation of all values. If the mean proportion of the vulnerable waters locations covered with mesic vegetation is high during these dry months, we consider this to be a well connected, intact system and relatively decoupled from climatic variability (Beechie et al., 2010; Cartwright and Johnson, 2018; Pollock et al., 2014).

2.4.3 Variability

We also calculated the coefficient of variation (CV) of the entire time series of each HUC12 unit, which we use as an inverse proxy for the ability of systems with at least middling intactness to withstand the dry season. Thus, we have reasoned that a low CV considered along with high intactness of a watershed can be indicative of the resilience, following the rationale that a system well connected and with a high late season wetted proportion is less sensitive to variance in annual precipitation inputs, and can function as a sponge rather than a conduit. These systems in theory are ultimately more resilient to regime shifts, maintaining baseflows and creating flow asynchronies necessary for watershed functions (Cartwright and Johnson, 2018; Lane et al., 2023; Moore et al., 2015). For HUC12 units where we observed peak mesic vegetation in July rather than June, we omitted June and September months from the record with the rationale that these were energy limited, as we anecdotally observed pixels classified as snow in September months at times, corroborating this hypothesis.

2.4.4 Sensitivity

Finally, we calculated the Spearman's rank correlation coefficient for intactness and a climate metric, the one year moving Standardized Precipitation Evapotranspiration Index produced by GRIDMET (Abatzoglou, 2013). We did this to demonstrate the sensitivity of a system to climate, where high values would indicate reduced stability and resilience to shocks. Quantifying absolute resilience would require intimate knowledge of each sub-basin, but estimating relative proxies of resilience of each HUC12 unit is both achievable and potentially useful for prioritization of restoration efforts (Dakos and Kéfi, 2022). Satellite time series, particularly over large geographic areas, often have missing data. We chose not to fill any gaps in the time series in favor of analyzing only HUC12 units with a complete time series for this demonstration, resulting in 14,439 of 18,861 units with complete observation records.

2.4.5 Prioritization example

To show how these indicators of watershed health can be used for prioritization, we mapped the three indicators for HUC12 units in an example HUC8 unit (17040213). If a manager was tasked with allocating limiting restoration funds, they could use the following maps to investigate possible locations for restoration projects. We mapped the indicators of vulnerable waters health in HUC12 units in an example HUC8 subbasin in the central part of our study area. We describe how we interpret the values of each indicator and show how these indicators could be useful for

identifying priority areas for restoration of vulnerable waters in a straightforward and logical Geographic Information System (GIS) workflow. We expect the workflow we present to be easily reproduced by potential end users with some familiarity with GIS tools and methods without requiring extensive geospatial expertise.

3. Results

3.1. Remote sensing classification

The overall accuracy of our classified maps ranges from 95.95% (± 2.78%) in July 2021 to 98.33% (± 1.62%) in August 2018 (Table 2). Estimated producer's accuracy (PA; the complement of omission error) for mesic vegetation ranges from 66.99% (± 25.01%) in September 2021 to 100% (± 0%) in June and July 2024. For surface water PA ranges from 29.69% (± 23.46%) in July 2021 to 100% (± 0%) in September 2021, June, July, and August 2024. For the 'other' class PA ranges from 95.49% (± 1.54%) in June 2024 to 99.75% (± 0.33%) in September 2018. These results demonstrate the impact of only a few misclassifications of rare classes on uncertainty and estimated PA, as the month with the lowest estimated PA for water, July 2021, had three misclassified water pixels (Table S6), committed to the 'other' class, which led to large decreases in estimated accuracy and increased uncertainty. Estimated user's accuracy (UA; the complement of commission error) for mesic vegetation range from 72.73% (± 10.01%) in June 2024 to 95.35% (± 6.37%) in July 2018. UA for water ranges from 92.31% in September 2024 (± 5.95%) to 100% in July 2018 (± 0%), and for the other class from 96.55% (± 2.98%) in July 2021 to 100% (± 0%) in June, July, and August of 2024.

Table 2. Area adjusted accuracy outputs for all models.

			Adjusted Area		Accuracy					
Year	*Month*	*Class*	*km²*	*km²±*	*PA*	*PA±*	*UA*	*UA±*	*OA*	*OA±*
2018	June	Other	1441575.42	34790.62	98.13	1.29	98.53	2.03	97.23	2.01
		Mesic	262889.07	28079.27	95.98	7.56	90.41	6.8		
		Water	28460.49	20695.04	62.91	45.74	98.9	2.15		
	July	Other	1508998.63	25981.38	98.38	1.13	99.34	1.3	98.02	1.49
		Mesic	212978.78	25981.38	95.35	8.69	89.23	7.59		
		Water	16862.39	0	100	0	100	0		
	August	Other	1589320	28139.58	99.38	0.57	98.8	1.66	98.33	1.62
		Mesic	127159.76	20967.97	92.43	13.73	92.45	7.18		
		Water	25256.93	18881.2	61.87	46.24	98.77	2.42		
	September	Other	1590405.01	35032.62	99.75	0.33	97.8	2.14	97.69	2.04

		Mesic	95275.58	25173.19	81.29	21.04	95.35	6.37		
		Water	32763.64	24639.03	45.6	34.29	98.67	2.61		
2021	June	Other	1526696.76	46536.03	98.98	0.67	96.99	2.91	96.4	2.68
		Mesic	181918.87	40771.68	80.68	17.54	90.48	6.32		
		Water	26350.76	22961.53	55.55	48.4	98.8	2.36		
	July	Other	1545718.68	48194.94	98.99	0.62	96.55	2.98	95.95	2.78
		Mesic	144138.71	31677.55	84.84	17.8	88.75	6.97		
		Water	46631.62	36844.56	29.69	23.46	98.67	2.61		
	August	Other	1602298.19	38801.98	99.15	0.53	97.6	2.33	96.96	2.24
		Mesic	107846.76	33963.18	72.89	22.33	85.71	9.25		
		Water	23139.27	19112.45	57.88	47.8	96.1	4.35		
	September	Other	1622136.57	32126.81	99.44	0.4	98.3	1.92	97.85	1.87
		Mesic	84728.95	32121.23	66.99	25.01	86.96	9.84		
		Water	13396.47	598.45	100	0	96.15	4.3		
2024	June	Other	1510699.81	24368.29	95.49	1.54	100	0	96.02	1.42
		Mesic	184745.02	24362.51	100	0	73.17	9.65		
		Water	16946.1	530.77	100	0	97.78	3.06		
	July	Other	1551368.78	21553.48	96.19	1.34	100	0	96.57	1.25
		Mesic	156505.39	21547.37	100	0	72.73	10.01		
		Water	15651.89	513.44	100	0	97.67	3.2		
	August	Other	1601414.26	16226.52	97.83	0.99	100	0	97.96	0.95
		Mesic	100198.11	16218.69	99.82	0.36	74.51	12.08		
		Water	14817.24	712.8	100	0	95.24	4.58		
	September	Other	1612568.18	27311.45	98.46	0.83	98.93	1.48	97.55	1.6
		Mesic	76835.84	21567.96	88.83	19.55	74.29	14.69		
		Water	22491.08	16845.81	61.84	46.28	92.31	5.95		

3.2 Functions of vulnerable waters

We analyzed 14,439 hydrologic unit code subwatersheds (HUC12) within 20 ecoregions that occur within the sagebrush biome. The number of HUC12 units in each ecoregion ranged from 56 (Arizona/New Mexico Mountains) to 2,119 (Central Basin and Range, Table 3). We demonstrate that the measures of central tendency show low levels of intactness of vulnerable waters throughout the sagebrush biome, although there are many outlying cases in every ecoregion (Figure 2A, Table 3). We observe the lowest mean and median intactness measures in the Mojave Basin and Range (0.0108; 0.0019), and the highest mean and median values in the Wasatch and Uinta Mountains (0.2967, 0.2741; Figure 2A, Table 3).

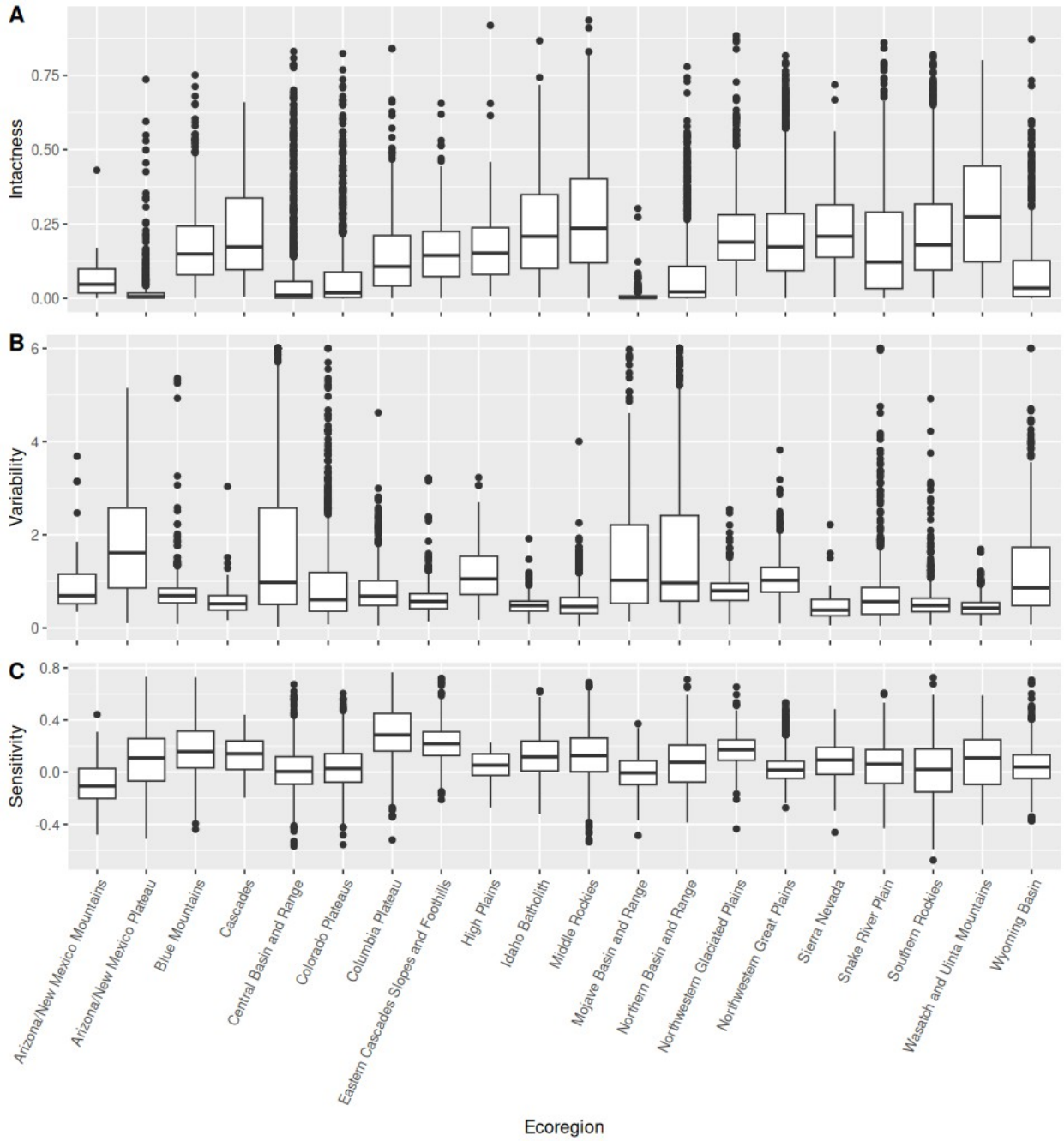

Figure 2. The distributions of A) the mean proportion of mesic vegetation in valley bottoms (Intactness), B) the coefficient of variation (Variability), and C) correlation between SPEI and mesic vegetation (Sensitivity) for HUC12s in EPA level III ecoregion.

Table 3. Counts of HUC12 units analyzed per ecoregion, intactness (mesic vegetation proportion of valley bottom, variability of mesic vegetation proportion (coefficient of variation), and sensitivity to climate (correlation coefficient with one year SPEI value). Blue indicates level III ecoregions that belong to Warm Desert and Upper Gila level II ecoregions, green belong to Western Cordillera, yellow to Cold Deserts, and orange to Plains.

		Intactness				**Variability**				**Sensitivity**			
Ecoregion	Count	Lower 95%	Mean	Median	Upper 95%	Lower 95%	Mean	Median	Upper 95%	Lower 95%	Mean	Median	Upper 95%
Arizona/New Mexico Mountains	56	0.0002	0.0682	0.0468	0.2267	0.3477	0.9467	0.6941	2.157	-0.4798	-0.0831	-0.107	0.3906
Arizona/New Mexico Plateau	681	0	0.0255	0.0057	0.0431	0.105	1.7853	1.6129	5.1522	-0.5111	0.1011	0.1091	0.7317
Blue Mountains	888	0	0.1731	0.1489	0.5019	0.0873	0.7365	0.6944	1.3486	-0.4127	0.1698	0.1573	0.7276
Cascades	106	0.0055	0.2203	0.173	0.6601	0.1683	0.5906	0.5209	1.1899	-0.1973	0.1431	0.1408	0.4409
Central Basin and Range	2119	0	0.0629	0.0103	0.1443	0.0312	1.6431	0.9801	5.8432	-0.4245	0.0145	0.0044	0.4512
Colorado Plateaus	1188	0	0.0815	0.0185	0.2234	0.0763	0.9467	0.6086	2.502	-0.4233	0.0369	0.0279	0.4887
Columbia Plateau	648	0.0002	0.1445	0.1067	0.4799	0.0514	0.8173	0.6834	1.856	-0.2932	0.2875	0.2854	0.7666
Eastern Cascades Slopes and Foothills	395	0	0.1603	0.1442	0.4644	0.1392	0.6367	0.5712	1.2456	-0.1584	0.217	0.2183	0.5957
High Plains	67	0.0078	0.1884	0.1518	0.487	0.179	1.1876	1.055	2.8426	-0.2703	0.0402	0.0535	0.2291
Idaho Batholith	457	0.0025	0.2364	0.2084	0.7416	0.0856	0.487	0.4832	0.9123	-0.323	0.1212	0.1166	0.6004
Middle Rockies	1507	0.0002	0.2736	0.2358	0.848	0.042	0.5161	0.4624	1.1954	-0.4045	0.1307	0.1269	0.6687
Mojave Basin and Range	213	0	0.0108	0.0019	0.0197	0.145	1.5741	1.0246	4.8666	-0.3857	-0.002	-0.0057	0.3713
Northern Basin and Range	1133	0	0.0855	0.0218	0.2731	0.0881	1.6036	0.9684	5.3088	-0.3866	0.0698	0.0767	0.6566
Northwestern Glaciated Plains	432	0.0081	0.2284	0.189	0.5217	0.0748	0.808	0.799	1.5428	-0.1557	0.1636	0.1717	0.4948
Northwestern Great Plains	1576	0.0001	0.2134	0.1731	0.5868	0.0958	1.042	1.0234	2.1319	-0.2555	0.0322	0.0167	0.2923
Sierra Nevada	92	0.004	0.2277	0.2084	0.5939	0.0586	0.4757	0.3837	1.1725	-0.3434	0.0798	0.0933	0.484
Snake River Plain	548	0	0.1872	0.1218	0.6951	0.0477	0.8034	0.5652	1.7735	-0.4311	0.0505	0.0616	0.5818
Southern Rockies	1055	0.0001	0.224	0.1793	0.6673	0.0644	0.5541	0.4831	1.096	-0.6718	0.0201	0.0207	0.6976
Wasatch and Uinta Mountains	405	0.0001	0.2967	0.2741	0.8016	0.053	0.454	0.4294	0.9285	-0.4026	0.0829	0.1094	0.5893
Wyoming Basin	873	0	0.0928	0.0343	0.3178	0.0716	1.2191	0.8608	3.7083	-0.3347	0.0451	0.0395	0.4199

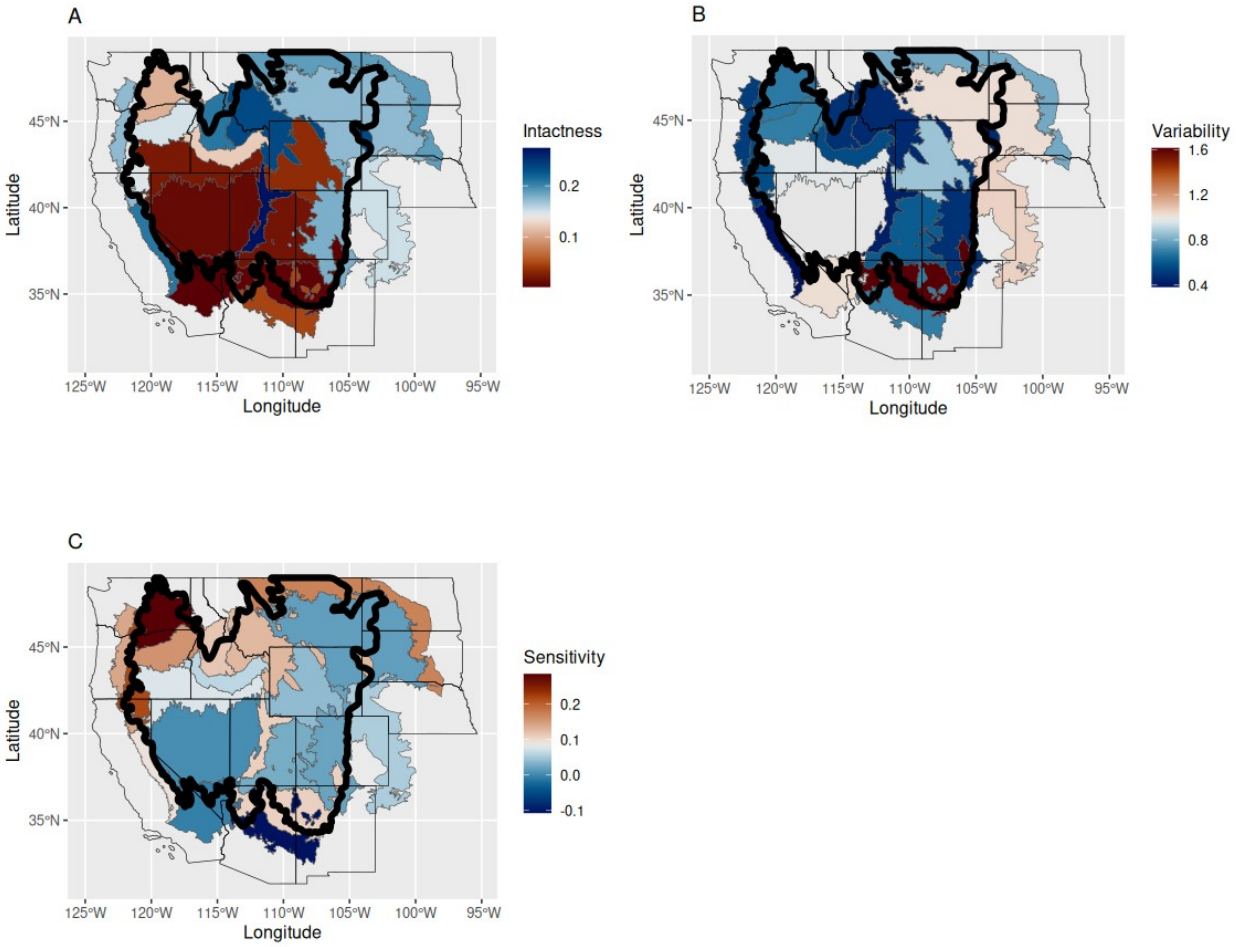

Figure 3. Median values of relative intactness (A), variability (B), and sensitivity (C) of vulnerable waters in ecoregions across the sagebrush biome.

We show the mean and median levels of variability of vulnerable waters within and among ecoregions vary substantially (Figure 2B, Figure 3). We observed the highest mean and median CV values in the Arizona/New Mexico Plateau ecoregion (1.79; 1.61) (Figure 2; Table 3). We observed both the lowest mean and median values in the Wasatch and Uinta Mountains (0.45, 0.43) (Figure 2B; Table 3). While these measures of central tendency generally follow along with theoretical variability, there are many outlying cases where systems are highly variable, particularly outside of mountainous ecoregions (Figures 2-4). Figure 4 shows the overall relationships of each ecoregion between intactness and variability, with wetter ecoregions showing steep declines in intactness as variability increases (e.g. Blue Mountains, Middle and Southern Rockies, etc.) and drier ecoregions showing low intactness values and consistently high variability measures (e.g. Arizona/New Mexico Mountains and Plateau, Mojave Basin and Range). Points in the upper tails of the distributions on the x-axis of plots in Figure 4 show HUC12 units that are extremely variable relative to their means. We see four shapes worth noting in these plots corresponding with Level II EPA ecoregions: the Western Cordillera (high

intactness intercept and low variability distribution), warm desert and Gila Mountains (monsoonal; low intactness and highly variable), Cold Desert (middling intactness and highly variable), and prairies (high intactness and middling variability), consistent with our understanding of these respective systems (Table 3; Figure 4).

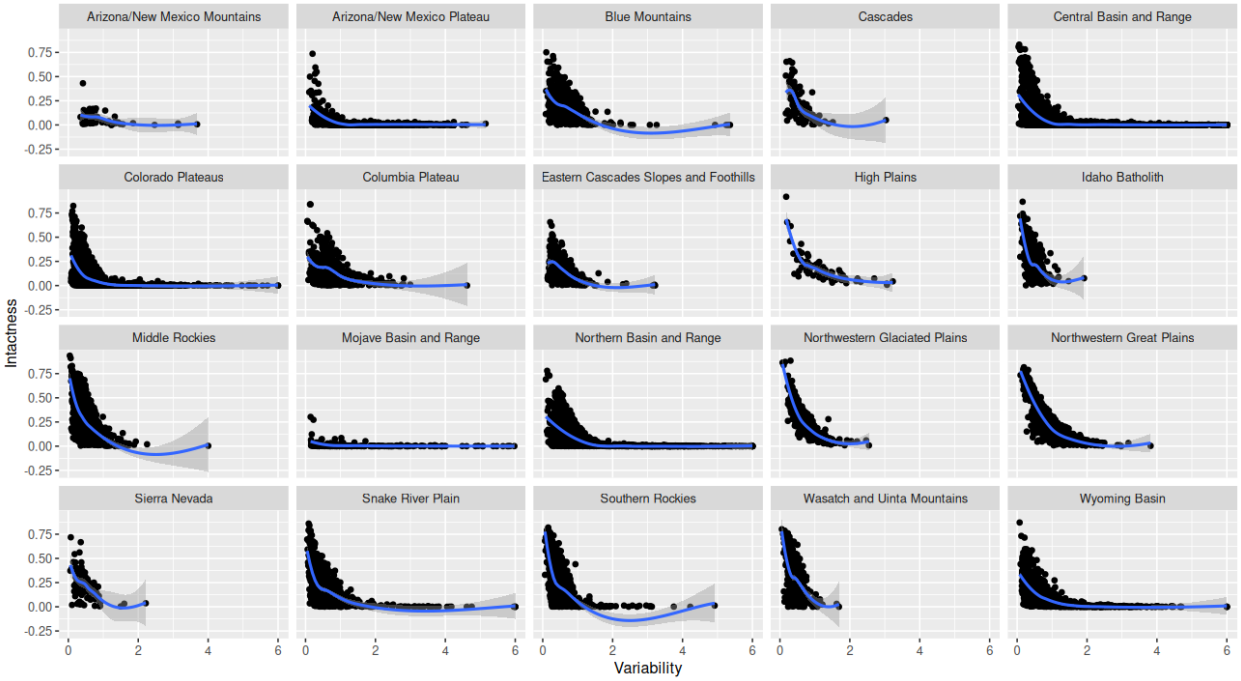

Figure 4. Plots of intactness and variability of each HUC12 for each ecoregion in the sagebrush biome. Blue lines are fitted loess regressions to show general relationships between the two indicators.

Finally, we demonstrate that the sensitivity of vulnerable waters to climate as measured by the one year SPEI is also highly variable throughout the study region. We found the ecoregion with the strongest association with climate as measured by both mean and median is the Columbia Plateau, both with values near 0.29 (Figure 2C; Table 3). We find that many ecoregions have low (near zero) mean and median association with the climate metrics indicating that water availability is driven by other factors in these systems (Figure 2C; Table 2). As we found with the other metrics, outlying watersheds in nearly every ecoregion show strong associations with climate, indicating a dependency of intactness on precipitation inputs in those subwatersheds (Figures 2,3). We demonstrate that HUC12 units that are the most variable are not always the most sensitive to the one-year SPEI value (Figure S2), and further show that in mountainous and northern ecoregions many of the most sensitive HUC12 units are also the most intact (Figure S3).

3.3 Prioritization example

We envision managers may start by looking at the HUC12 units with very low intactness (Figure 5A) as possible targets. If any of these with ‘low’ intactness also have low variability (Figure 5B), that could indicate a watershed in poor condition regardless of the season but may require a big lift, or may not be a particularly good target for restoration for other reasons (e.g. human infrastructure). Alternatively, if a HUC12 unit has low/medium intactness and high variability, this

might mean that the channel is disconnected from the floodplain, but some restoration activities could restore the connection, ultimately increasing intactness and reducing the variability of available water throughout the system. If intactness and variability indicators of HUC12 units are middling but show a strong sensitivity to climate (Figure 5C), these may be good targets for restoration since they are likely susceptible to disturbances such as drought and wildfire events that could degrade them further. Of other considerations a manager may want to investigate is the density (total area in km^2 of vulnerable waters, Figure 5D) that might help identify units with the most vulnerable waters area. They might also choose to refer to the National Land Cover dataset (Figure 5E) to determine whether these areas are good targets relative to human development (e.g. agriculture, urban areas).

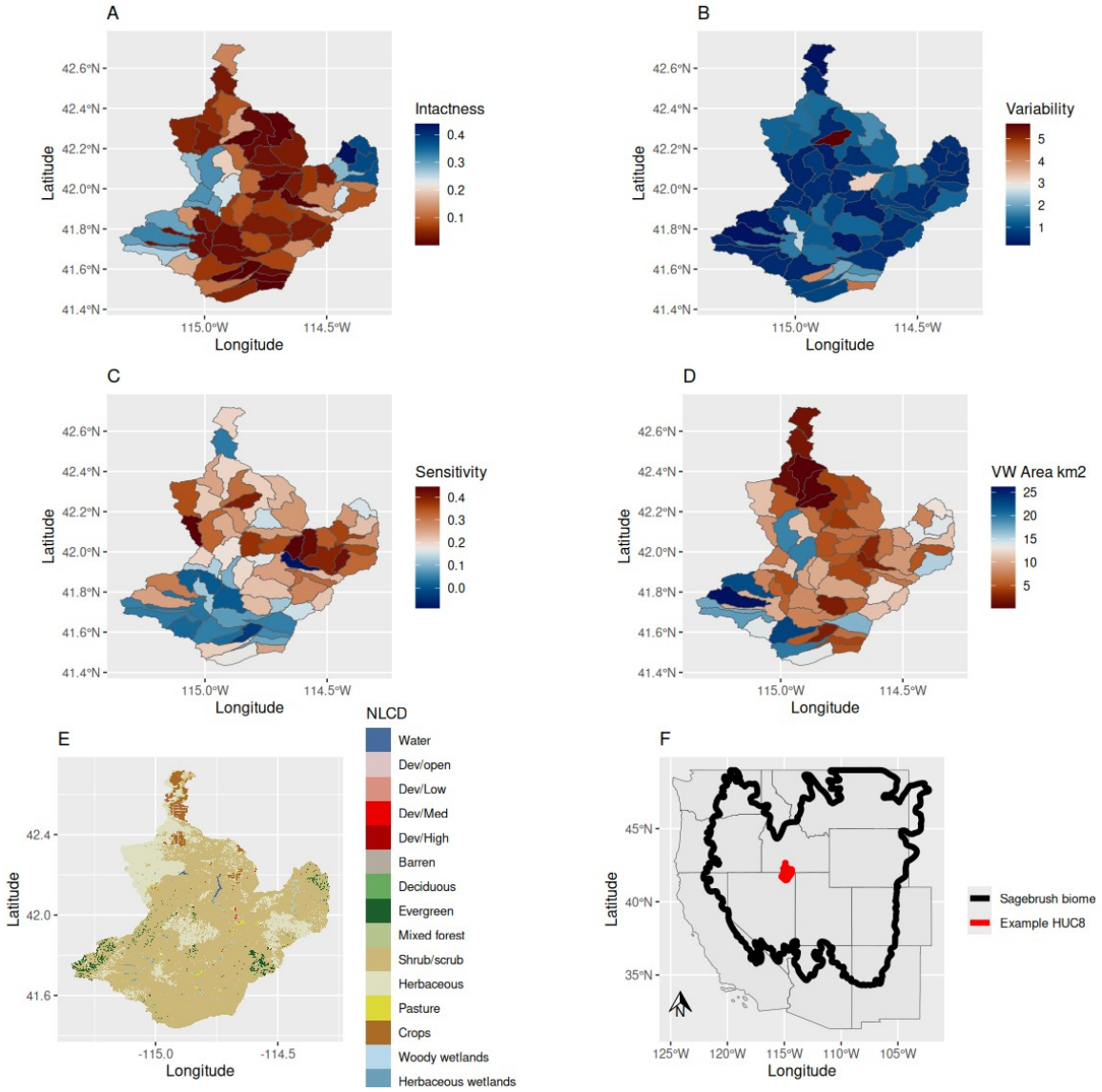

Figure 5. Examples of A) intactness, B) variability, C) sensitivity, D) density of vulnerable waters (VW), and E) the National Land Cover Dataset for reference for HUC12 units in an example HUC8 subbasin in the central part of the study area (F)).

4. Discussion

4.1 Mapping vulnerable waters from space

Our analyses demonstrate the utility of intra-annual time series classifications for identifying potential degradation in headwater systems. The classification approach we take circumvents common drawbacks of index approaches such as saturation common to the use of NDVI (Liu et al., 2012), or determination of a threshold for maps of continuous measures (Shrestha et al., 2024). We also show how the mode of classifications of all images captured in a month can produce reliable intra-annual information necessary for gleaning insights into the dynamics of systems that are inherently variable (Brudvig et al., 2017; Lengyel et al., 2020). We use these intra-annual measurements to help identify targets for restoration given the current state of intactness and variability. We also envision these time series could be useful for monitoring and assessing efficacy following restoration efforts by identifying shifts in the time series of intactness and variability towards a more desirable state (Kolarik et al., 2025b).

4.2 Scaling and perspectives

We acknowledge that although we developed our tools for all dryland regions across the sagebrush biome, there is substantial variation among these ecoregions in terms of their infrastructure, inputs, and functions. It is unrealistic to expect “one-size-fits-all” recommendations across these disparate ecoregions and we suggest that managers use relative measures within ecoregions to identify potential restoration targets to determine appropriate reference conditions (Hiers et al., 2012; Shackelford et al., 2024). For example, choosing HUC12 units with low intactness is a logical place to start for prioritizing restoration, but we have shown that even the highest levels of intactness in the most arid ecoregions are far lower than many of those in wetter ecoregions, and the reference conditions must be considered regionally as underlying geologies complicate comparisons across them (Albano et al., 2020). In other words, regional management efforts are constrained by unique regional parameters and should be supported by regional strategies and datasets (Wyborn et al., 2019). We demonstrate that HUC12 dynamics vary based on the ecoregion and strategies for prioritization would need to vary accordingly. For example, It is unreasonable to expect vulnerable waters in hyper-arid regions to have intactness comparable to relatively wet plains regions. It would take further, region specific, investigation to reveal whether these systems are degraded or whether the low intactness is an artifact of more ephemeral systems in arid environments (Albano et al., 2020). Using a regional approach further opens up the opportunity to use finer scale valley bottom boundaries, such as those derived from aerial lidar, and thus increasing the precision of estimates of riverscape functions (Glassic et al., 2024).

4.3 Supporting information and context

It may also be helpful to consider other datasets to help guide restoration prioritization as multiple goals may be of interest. An obvious contender in the sagebrush biome is the Sagebrush Conservation Design (Doherty et al., 2022) which evaluates the health of the dominant ecosystem, the sagebrush steppe. Another dataset that is relevant to the restoration

of vulnerable waters would be the Beaver Restoration Assessment Tool (BRAT) identifying locations where low-tech process-based restoration has high potential of success (Macfarlane et al., 2017b). Personal communications with our end users have revealed that using the intactness and variability measures in combination with other datasets have been useful for identifying targets. Although we were unable to do so over such a large heterogeneous geography due to aforementioned differences among systems mapped, they were able to use local knowledge and context to develop a single metric for identifying potential restoration sites. Some systems may be in biophysical states that are too far removed from their reference condition and/or encumbered by human infrastructure. These systems should not be considered as good contenders for restoration and prioritization of locations with high likelihood of success is paramount (Skidmore and Wheaton, 2022).

4.4 Varying effects of climate and geology

We found relatively low levels of ecologically available water in vulnerable waters in the driest months of the water year throughout the sagebrush biome. The relatively low proportions of valley bottoms occupied by mesic vegetation is an indicator that many valley bottoms are poorly connected with their floodplains, which suggests the delivery of the functions provided by vulnerable waters are greatly limited (Lane et al., 2023). In theory, their minimum extents are defined by shallow groundwater and baseflows, and should not show strong responses to intra- and interannual climatic variation (Albano et al., 2020; Glassic et al., 2024). Our data indicate that extents of vulnerable waters in many HUC12s are sometimes highly variable and climate dependent, but these do not always co-occur. In fact, we observe an inverse relationship in mountainous and northern regions, where the most sensitive HUC12 units are also the most intact. While this aligns with observations that the greening of the Earth is occurring preferentially at northern and high elevation areas (Macek et al., 2025), it is not intuitive and not often discussed in middling latitudes and elevations. It could be possible that the drought metric we chose, the one-year SPEI, is not always appropriate, as groundwater is often the main control of baseflows storage times vary widely across space (Brooks et al., 2025). These results deserve more investigation to elucidate the drivers of variability if not climate, as estimating the ability of the natural infrastructure to mitigate disturbances in the land system has never been more relevant.

4.5 Policy and management implications

When we aggregate the indicators of intactness, variability, and sensitivity to the ecoregion level the values tend to converge, but some measures stand out as particularly alarming. First, the Columbia Plateau, a region with a high proportion of agriculture, shows high sensitivity to climate. Though a more formal analysis is needed to rigorously investigate, agricultural conversions often come at the expense of vulnerable waters and programs that seek to restore ecological functions of agricultural land could help to reverse this possible degradation (Ahmed and Jackson-Smith, 2019; Braza, 2017). Ecoregions with high proportions of agriculture typically have less federally managed land, indicating that many of the at-risk vulnerable waters may be under private ownership, and thus there are limited options for federal protection, policy, and

management (Joppa and Pfaff, 2009). While various options for voluntary private lands conservation focused on vulnerable waters, their outcomes are mixed (Brown et al., 2022; Kolarik et al., 2025a). It has long been documented that private land conservation is integral to meeting biodiversity targets and our findings corroborate the need to focus on protection of highly productive non-federal lands (Brown et al., 2022; Kolarik et al., 2025a; Rissman et al., 2007).

Overallocated water budgets have exacerbated changes in the water supply in the West in ways that are unsustainable (Gleick, 2010). Datasets and metrics like the ones we present here are important for elucidating potential loss of keystone landscape features like vulnerable waters and determining priority areas to mitigate these losses (Donnelly et al., 2020; Pilliod et al., 2022). The impacts of the changes humanity has made to the system, some of which were intended to make water management and supply more straightforward, degrade the functions capable of dampening the effects of drought and wildfire (Allan et al., 2020; Gleick, 2010). Now that researchers better understand the processes that these systems support, and acknowledge the hydrologic inefficiency is favorable for high functioning systems, we are better positioned to renovate systems to elevate the functions they provide (Dewey et al., 2022; Prober et al., 2019). Ecosystems are dynamic and variable, but every system has limits and historical ranges of variability that support ecosystem processes are increasingly exceeded (Hiers et al., 2012). Through this work we provide some evidence that the many of vulnerable waters in watersheds across the semi-arid West may have exceeded a range of variability able to support ecosystem processes, which in aggregate leaves the water system, and the functions and populations it supports, at great risk (Lane et al., 2023). The dynamics of these metrics could also help to glean insights to surface water availability by assisting in its prediction and identifying drivers of change (Vanderhoof et al., 2025). Given these capabilities, we envision the dataset we have introduced in this study is well poised to support more holistic ecosystem-based management that rivers need to meet biodiversity targets, as well as the allocation of limited conservation resources across space and jurisdictional boundaries (Gleick, 2010).

4.6 Future directions

The detailed dataset of vulnerable waters condition and change we present provides avenues for future important research. We demonstrate the utility of the dataset we introduce here for high level metrics and signals of change throughout this dynamic region. However, we acknowledge that we are merely scratching the surface of what is possible with these data. For example, we aggregate these data to produce HUC12 level metrics, but there may be processes of interest that occur at finer or coarser scales worthy of investigation. The spatial arrangements of vulnerable waters have been shown to be of particular importance for attenuating peak flows and maintaining baseflows in the prairie pothole region (Evenson et al., 2018b). These maps could integrate landscape ecology metrics in similar ways to identify how connectivity, patch size, distance between patches, etc. affect discharge, groundwater availability, biodiversity, and biogeochemical flows. Linking these data to *in situ* data collection efforts will further highlight their utility, as all products derived from remotely sensed information are limited to some degree. Though we introduce these data by identifying ecoregion indicators,

we envision these data are useful for prioritization of restoration treatments to meet biodiversity goals across all levels of the system (Cid et al., 2022). Targeting watersheds identified using resilience indicators while also integrating landscape ecology metrics such as patch connectivity could help to effectively target areas in need and link source and sink populations (Jaeger et al., 2014). These metrics could further be assessed across adjacent units to address higher levels of the meta-system (Rayden et al., 2023).

5. Conclusions

Remotely sensed data and derived products are useful for mapping and monitoring across large swaths of space and time, though are mostly limited to high level biophysical processes. The time series classifications we present is a relevant proxy for the dynamics of ecologically available water across a large portion of the dryland western U.S. These data are derived from freely available datasets and are made publicly available via our Google Earth Engine application and Climate Engine (Huntington et al., 2017). We encourage others to use them for investigations of system changes throughout the West and make use of our open source code for applications to other regions.

Acknowledgements: We thank Charles Lane for his support and insights that helped shape this manuscript. We are also grateful for funding support from USDA Data Science for Food and Agriculture Systems 2022-11619 and NASA Ecological Forecasting Applied Sciences 80NSSC21K1642.

GEE repository: https://code.earthengine.google.com/?accept_repo=users/nekolarik/SentSage
Github: https://github.com/neko1010/watershedResilience

6. References

Abatzoglou, J.T., 2013. Development of gridded surface meteorological data for ecological applications and modelling. Int. J. Climatol. 33, 121–131. https://doi.org/10.1002/joc.3413

Abatzoglou, J.T., Williams, A.P., 2016. Impact of anthropogenic climate change on wildfire across western US forests. Proc. Natl. Acad. Sci. 113, 11770–11775. https://doi.org/10.1073/pnas.1607171113

Ahmed, S., Jackson-Smith, D., 2019. Impacts of Spatial Patterns of Rural and Exurban Residential Development on Agricultural Trends in the Intermountain West. SAGE Open 9, 2158244019871037. https://doi.org/10.1177/2158244019871037

Albano, C.M., McGwire, K.C., Hausner, M.B., McEvoy, D.J., Morton, C.G., Huntington, J.L., 2020. Drought Sensitivity and Trends of Riparian Vegetation Vigor in Nevada, USA (1985–2018). Remote Sens. 12, 1362. https://doi.org/10.3390/rs12091362

Allan, R.P., Barlow, M., Byrne, M.P., Cherchi, A., Douville, H., Fowler, H.J., Gan, T.Y., Pendergrass, A.G., Rosenfeld, D., Swann, A.L.S., Wilcox, L.J., Zolina, O., 2020. Advances in understanding large-scale responses of the water cycle to climate change. Ann. N. Y. Acad. Sci. 1472, 49–75. https://doi.org/10.1111/nyas.14337

Beechie, T.J., Sear, D.A., Olden, J.D., Pess, G.R., Buffington, J.M., Moir, H., Roni, P., Pollock, M.M., 2010. Process-based Principles for Restoring River Ecosystems. BioScience 60, 209–222. https://doi.org/10.1525/bio.2010.60.3.7

Behnamian, A., Banks, S., White, L., Brisco, B., Millard, K., Pasher, J., Chen, Z., Duffe, J., Bourgeau-Chavez, L., Battaglia, M., 2017. Semi-Automated Surface Water Detection with Synthetic Aperture Radar Data: A Wetland Case Study. Remote Sens. 9, 1209. https://doi.org/10.3390/rs9121209

Belgiu, M., Drăguţ, L., 2016. Random forest in remote sensing: A review of applications and future directions. ISPRS J. Photogramm. Remote Sens. 114, 24–31. https://doi.org/10.1016/j.isprsjprs.2016.01.011

Belote, R.T., Barnett, K., Dietz, M.S., Burkle, L., Jenkins, C.N., Dreiss, L., Aycrigg, J.L., Aplet, G.H., 2021. Options for prioritizing sites for biodiversity conservation with implications for “30 by 30.” Biol. Conserv. 264, 109378. https://doi.org/10.1016/j.biocon.2021.109378

Braza, M., 2017. Effectiveness of conservation easements in agricultural regions. Conserv. Biol. 31, 848–859. https://doi.org/10.1111/cobi.12909

Brooks, P.D., Solomon, D.K., Kampf, S., Warix, S., Bern, C., Barnard, D., Barnard, H.R., Carling, G.T., Carroll, R.W.H., Chorover, J., Harpold, A., Lohse, K., Meza, F., McIntosh, J., Neilson, B., Sears, M., Wolf, M., 2025. Groundwater dominates snowmelt runoff and controls streamflow efficiency in the western United States. Commun. Earth Environ. 6, 1–8. https://doi.org/10.1038/s43247-025-02303-3

Brown, S.A., Rotman, R.M., Powell, M.A., Wilhelm Stanis, S.A., 2022. Conservation easements: A tool for preserving wildlife habitat on private lands. Wildl. Soc. Bull. n/a, e1415. https://doi.org/10.1002/wsb.1415

Brudvig, L.A., Barak, R.S., Bauer, J.T., Caughlin, T.T., Laughlin, D.C., Larios, L., Matthews, J.W., Stuble, K.L., Turley, N.E., Zirbel, C.R., 2017. Interpreting variation to advance predictive restoration science. J. Appl. Ecol. 54, 1018–1027. https://doi.org/10.1111/1365-2664.12938

Bwangoy, J.-R.B., Hansen, M.C., Roy, D.P., Grandi, G.D., Justice, C.O., 2010. Wetland mapping in the Congo Basin using optical and radar remotely sensed data and derived topographical indices. Remote Sens. Environ. 114, 73–86. https://doi.org/10.1016/j.rse.2009.08.004

Cartwright, J., Johnson, H.M., 2018. Springs as hydrologic refugia in a changing climate? A remote-sensing approach. Ecosphere 9, e02155. https://doi.org/10.1002/ecs2.2155

Castellazzi, P., Doody, T., Peeters, L., 2019. Towards monitoring groundwater-dependent ecosystems using synthetic aperture radar imagery. Hydrol. Process. 33, 3239–3250. https://doi.org/10.1002/hyp.13570

Christensen, J.R., Golden, H.E., Alexander, L.C., Pickard, B.R., Fritz, K.M., Lane, C.R., Weber, M.H., Kwok, R.M., Keefer, M.N., 2022. Headwater streams and inland wetlands: Status and advancements of geospatial datasets and maps across the United States. Earth-Sci. Rev. 235, 104230. https://doi.org/10.1016/j.earscirev.2022.104230

Cid, N., Erős, T., Heino, J., Singer, G., Jähnig, S.C., Cañedo-Argüelles, M., Bonada, N., Sarremejane, R., Mykrä, H., Sandin, L., Paloniemi, R., Varumo, L., Datry, T., 2022. From meta-system theory to the sustainable management of rivers in the Anthropocene. Front. Ecol. Environ. 20, 49–57. https://doi.org/10.1002/fee.2417

Creed, I.F., Lane, C.R., Serran, J.N., Alexander, L.C., Basu, N.B., Calhoun, A.J.K., Christensen, J.R., Cohen, M.J., Craft, C., D’Amico, E., DeKeyser, E., Fowler, L., Golden, H.E., Jawitz, J.W., Kalla, P., Kirkman, L.K., Lang, M., Leibowitz, S.G., Lewis, D.B., Marton, J., McLaughlin, D.L., Raanan-Kiperwas, H., Rains, M.C., Rains, K.C., Smith, L., 2017. Enhancing protection for vulnerable waters. Nat. Geosci. 10, 809–815. https://doi.org/10.1038/ngeo3041

Dakos, V., Kéfi, S., 2022. Ecological resilience: what to measure and how. Environ. Res. Lett. 17, 043003. https://doi.org/10.1088/1748-9326/ac5767

Daly, C., Bryant, K., 2013. The PRISM Climate and Weather System – An Introduction.

Dewey, C., Fox, P.M., Bouskill, N.J., Dwivedi, D., Nico, P., Fendorf, S., 2022. Beaver dams overshadow climate extremes in controlling riparian hydrology and water quality. Nat. Commun. 13, 6509. https://doi.org/10.1038/s41467-022-34022-0

Doherty, K., Theobald, D.M., Bradford, J.B., Wiechman, L.A., Bedrosian, G., Boyd, C.S., Cahill, M., Coates, P.S., Creutzburg, M.K., Crist, M.R., Finn, S.P., Kumar, A.V., Littlefield, C.E., Maestas, J.D., Prentice, K.L., Prochazka, B.G., Remington, T.E., Sparklin, W.D., Tull, J.C., Wurtzebach, Z., Zeller, K.A., 2022. A sagebrush conservation design to proactively restore America's sagebrush biome (No. 2022–1081), Open-File Report. U.S. Geological Survey. https://doi.org/10.3133/ofr20221081

Doherty, K.E., Maestas, J., Remington, T., Naugle, D.E., Boyd, C., Wiechman, L., Bedrosian, G., Cahill, M., Coates, P., Crist, M., Holdrege, M.C., Kumar, A.V., Mozelewski, T., O'Connor, R.C., Olimpi, E.M., Olsen, A., Prochazka, B.G., Reinhardt, J.R., Smith, J.T., Sparklin, W.D., Theobald, D.M., Wollstein, K., 2024. State of the Sagebrush: Implementing the Sagebrush Conservation Design to Save a Biome. Rangel. Ecol. Manag., Defend and Grow the Core: Implementing the Sagebrush Conservation Design to Save a Biome 97, 1–11. https://doi.org/10.1016/j.rama.2024.08.017

Donnelly, J.P., King, S.L., Silverman, N.L., Collins, D.P., Carrera-Gonzalez, E.M., Lafón-Terrazas, A., Moore, J.N., 2020. Climate and human water use diminish wetland networks supporting continental waterbird migration. Glob. Change Biol. 26, 2042–2059. https://doi.org/10.1111/gcb.15010

Donnelly, J.P., Naugle, D.E., Hagen, C.A., Maestas, J.D., 2016. Public lands and private waters: scarce mesic resources structure land tenure and sage-grouse distributions. Ecosphere 7, e01208. https://doi.org/10.1002/ecs2.1208

European Commission (Ed.), 2023. GHSL data package 2023. Publications Office, Luxembourg. https://doi.org/10.2760/20212

European Space Agency, 2022. Mission ends for Copernicus Sentinel-1B satellite [WWW Document]. URL https://www.esa.int/Applications/Observing_the_Earth/Copernicus/Sentinel-1/Mission_ends_for_Copernicus_Sentinel-1B_satellite (accessed 5.7.25).

Evenson, G.R., Golden, H.E., Lane, C.R., McLaughlin, D.L., D'Amico, E., 2018a. Depressional wetlands affect watershed hydrological, biogeochemical, and ecological functions. Ecol. Appl. 28, 953–966. https://doi.org/10.1002/eap.1701

Evenson, G.R., Golden, H.E., Lane, C.R., McLaughlin, D.L., D'Amico, E., 2018b. Depressional wetlands affect watershed hydrological, biogeochemical, and ecological functions. Ecol. Appl. 28, 953–966. https://doi.org/10.1002/eap.1701

Fremier, A.K., Kiparsky, M., Gmur, S., Aycrigg, J., Craig, R.K., Svancara, L.K., Goble, D.D., Cosens, B., Davis, F.W., Scott, J.M., 2015. A riparian conservation network for ecological resilience. Biol. Conserv. 191, 29–37. https://doi.org/10.1016/j.biocon.2015.06.029

Glassic, H.C., McGwire, K.C., Macfarlane, W.W., Rasmussen, C., Bouwes, N., Wheaton, J.M., Al-Chokhachy, R., 2024. From pixels to riverscapes: How remote sensing and geospatial tools can prioritize riverscape restoration at multiple scales. WIREs Water n/a, e1716. https://doi.org/10.1002/wat2.1716

Gleick, P.H., 2010. Roadmap for sustainable water resources in southwestern North America. Proc. Natl. Acad. Sci. 107, 21300–21305. https://doi.org/10.1073/pnas.1005473107

Hale, K.E., Jennings, K.S., Musselman, K.N., Livneh, B., Molotch, N.P., 2023. Recent decreases in snow water storage in western North America. Commun. Earth Environ. 4, 1–11. https://doi.org/10.1038/s43247-023-00751-3

Hansen, M.C., Potapov, P.V., Pickens, A., Tyukavina, A., Hernandez Serna, A., Zalles, V., Turubanova, S., Kommareddy, I., Stehman, S.V., Song, X., Kommareddy, A., 2021. Global land use extent and dispersion within natural land cover using Landsat data. Environ. Res. Lett. https://doi.org/10.1088/1748-9326/ac46ec

Hiers, J.K., Mitchell, R.J., Barnett, A., Walters, J.R., Mack, M., Williams, B., Sutter, R., 2012. The Dynamic Reference Concept: Measuring Restoration Success in a Rapidly Changing No-Analogue Future. Ecol. Restor. 30, 27–36.

Holling, C.S., 1973. Resilience and Stability of Ecological Systems. Annu. Rev. Ecol. Syst. 4, 1–23. https://doi.org/10.1146/annurev.es.04.110173.000245

Hoylman, Z.H., 2021. A 30m Topographic Wetness Index Dataset for the Continental United States. https://doi.org/10.5281/zenodo.4460354

Hu, Y., Zhang, Q., Hu, S., Xiao, G., Chen, X., Wang, J., Qi, Y., Zhang, L., Han, L., 2022. Research progress and prospects of ecosystem carbon sequestration under climate change (1992–2022). Ecol. Indic. 145, 109656. https://doi.org/10.1016/j.ecolind.2022.109656

Huntington, J.L., Hegewisch, K.C., Daudert, B., Morton, C.G., Abatzoglou, J.T., McEvoy, D.J., Erickson, T., 2017. Climate Engine: Cloud Computing and Visualization of Climate and Remote Sensing Data for Advanced Natural Resource Monitoring and Process Understanding. Bull. Am. Meteorol. Soc. 98, 2397–2410. https://doi.org/10.1175/BAMS-D-15-00324.1

Jaeger, K.L., Olden, J.D., Pelland, N.A., 2014. Climate change poised to threaten hydrologic connectivity and endemic fishes in dryland streams. Proc. Natl. Acad. Sci. 111, 13894–13899. https://doi.org/10.1073/pnas.1320890111

Jin, H., Stehman, S.V., Mountrakis, G., 2014. Assessing the impact of training sample selection on accuracy of an urban classification: a case study in Denver, Colorado. Int. J. Remote Sens. 35, 2067–2081. https://doi.org/10.1080/01431161.2014.885152

Joppa, L.N., Pfaff, A., 2009. High and Far: Biases in the Location of Protected Areas. PLOS ONE 4, e8273. https://doi.org/10.1371/journal.pone.0008273

Ketchum, D., Jencso, K., Maneta, M.P., Melton, F., Jones, M.O., Huntington, J., 2020. IrrMapper: A Machine Learning Approach for High Resolution Mapping of Irrigated Agriculture Across the Western U.S. Remote Sens. 12, 2328. https://doi.org/10.3390/rs12142328

Kolarik, N.E., Cattau, M., Koehn, C., Roopsind, A., Williamson, M., Brandt, J., 2025a. Conservation easements target high quality lands but do not increase their quality. Biol. Conserv. 308, 111234. https://doi.org/10.1016/j.biocon.2025.111234

Kolarik, N.E., Koehn, C., Nati-Johnson, E., Rojas Lucero, J.C., Martin, C., Caughlin, T.T., Iskin, E., Jochems, L., Neville, H., Brandt, J., 2025b. Time series analysis to demonstrate restoration outcomes and system change from satellite data. Restor. Ecol. e70184. https://doi.org/10.1111/rec.70184

Kolarik, N.E., Roopsind, A., Pickens, A., Brandt, J.S., 2023. A satellite-based monitoring system for quantifying surface water and mesic vegetation dynamics in a semi-arid region. Ecol. Indic. 147, 109965. https://doi.org/10.1016/j.ecolind.2023.109965

Kornelsen, K.C., Coulibaly, P., 2013. Advances in soil moisture retrieval from synthetic aperture radar and hydrological applications. J. Hydrol. 476, 460–489. https://doi.org/10.1016/j.jhydrol.2012.10.044

Lane, C.R., Creed, I.F., Golden, H.E., Leibowitz, S.G., Mushet, D.M., Rains, M.C., Wu, Q., D'Amico, E., Alexander, L.C., Ali, G.A., Basu, N.B., Bennett, M.G., Christensen, J.R., Cohen, M.J., Covino, T.P., DeVries, B., Hill, R.A., Jencso, K., Lang, M.W., McLaughlin, D.L., Rosenberry, D.O., Rover, J., Vanderhoof, M.K., 2023a. Vulnerable Waters are Essential to Watershed Resilience. Ecosystems 26, 1–28. https://doi.org/10.1007/s10021-021-00737-2

Lane, C.R., D'Amico, E., Christensen, J.R., Golden, H.E., Wu, Q., Rajib, A., 2023c. Mapping global non-floodplain wetlands. Earth Syst. Sci. Data 15, 2927–2955. https://doi.org/10.5194/essd-15-2927-2023

Lane, C.R., Nahlik, A.M., Christensen, J., Golden, H., Dumelle, M., D'Amico, E., Olsen, A.R., 2025. Non-Floodplain Wetlands Are Carbon-Storage Powerhouses Across the United States. Earths Future 13, e2024EF005594. https://doi.org/10.1029/2024EF005594

Lehner, B., Verdin, K., Jarvis, A., 2008. New Global Hydrography Derived From Spaceborne Elevation Data. Eos Trans. Am. Geophys. Union 89, 93–94. https://doi.org/10.1029/2008EO100001

Lengyel, S., Mester, B., Szabolcs, M., Szepesváry, C., Szabó, G., Polyák, L., Boros, Z., Mizsei, E., Málnás, K., Mérő, T.O., Aradi, C., 2020. Restoration for variability: Emergence of the habitat diversity paradigm in terrestrial ecosystem restoration. Restor. Ecol. n/a. https://doi.org/10.1111/rec.13218

Liu, F., Qin, Q., Zhan, Z., 2012. A novel dynamic stretching solution to eliminate saturation effect in NDVI and its application in drought monitoring. Chin. Geogr. Sci. 22, 683–694. https://doi.org/10.1007/s11769-012-0574-5

Macek, M., Prošek, J., Doležal, J., Wild, J., Ježek, V., Kopecký, M., 2025. Elevation-dependent sensitivity of spectral greening to temperature and precipitation in the Western Himalayas. Environ. Res. Lett. 20, 054078. https://doi.org/10.1088/1748-9326/adc9c7

Macfarlane, W.W., Gilbert, J.T., Jensen, M.L., Gilbert, J.D., Hough-Snee, N., McHugh, P.A., Wheaton, J.M., Bennett, S.N., 2017a. Riparian vegetation as an indicator of riparian condition: Detecting departures from historic condition across the North American West. J. Environ. Manage. 202, 447–460. https://doi.org/10.1016/j.jenvman.2016.10.054

Macfarlane, W.W., Wheaton, J.M., Bouwes, N., Jensen, M.L., Gilbert, J.T., Hough-Snee, N., Shivik, J.A., 2017b. Modeling the capacity of riverscapes to support beaver dams. Geomorphology 277, 72–99. https://doi.org/10.1016/j.geomorph.2015.11.019

Maestas, J.D., Knight, R.L., Gilgert, W.C., 2001. Biodiversity and Land-Use Change in the American Mountain West. Geogr. Rev. 91, 509–524. https://doi.org/10.1111/j.1931-0846.2001.tb00238.x

Maestas, J.D., Porter, M., Cahill, M., Twidwell, D., 2022. Defend the core: Maintaining intact rangelands by reducing vulnerability to invasive annual grasses. Rangelands, Changing with the range: Striving for ecosystem resilience in the age of invasive annual grasses 44, 181–186. https://doi.org/10.1016/j.rala.2021.12.008

Margono, B.A., Bwangoy, J.-R.B., Potapov, P.V., Hansen, M.C., 2014. Mapping wetlands in Indonesia using Landsat and PALSAR data-sets and derived topographical indices. Geo-Spat. Inf. Sci. 17, 60–71. https://doi.org/10.1080/10095020.2014.898560

Marton, J.M., Creed, I.F., Lewis, D.B., Lane, C.R., Basu, N.B., Cohen, M.J., Craft, C.B., 2015. Geographically Isolated Wetlands are Important Biogeochemical Reactors on the Landscape. BioScience 65, 408–418. https://doi.org/10.1093/biosci/biv009

Moore, J.W., Beakes, M.P., Nesbitt, H.K., Yeakel, J.D., Patterson, D.A., Thompson, L.A., Phillis, C.C., Braun, D.C., Favaro, C., Scott, D., Carr-Harris, C., Atlas, W.I., 2015. Emergent stability in a large, free-flowing watershed. Ecology 96, 340–347. https://doi.org/10.1890/14-0326.1

Mozelewski, T.G., Freeman, P.T., Kumar, A.V., Naugle, D.E., Olimpi, E.M., Morford, S.L., Jeffries, M.I., Pilliod, D.S., Littlefield, C.E., McCord, S.E., Wiechman, L.A., Kachergis, E.J., Doherty, K.E., 2024. Closing the Conservation Gap: Spatial Targeting and Coordination are Needed for Conservation to Keep Pace with Sagebrush Losses. Rangel. Ecol. Manag., Defend and Grow the Core: Implementing the Sagebrush Conservation Design to Save a Biome 97, 12–24. https://doi.org/10.1016/j.rama.2024.08.016

Mushet, D.M., Alexander, L.C., Bennett, M., Schofield, K., Christensen, J.R., Ali, G., Pollard, A., Fritz, K., Lang, M.W., 2019. Differing Modes of Biotic Connectivity within Freshwater Ecosystem Mosaics. JAWRA J. Am. Water Resour. Assoc. 55, 307–317. https://doi.org/10.1111/1752-1688.12683

Olofsson, P., Foody, G.M., Herold, M., Stehman, S.V., Woodcock, C.E., Wulder, M.A., 2014. Good practices for estimating area and assessing accuracy of land change. Remote Sens. Environ. 148, 42–57. https://doi.org/10.1016/j.rse.2014.02.015

Olofsson, P., Foody, G.M., Stehman, S.V., Woodcock, C.E., 2013. Making better use of accuracy data in land change studies: Estimating accuracy and area and quantifying uncertainty using stratified estimation. Remote Sens. Environ. 129, 122–131. https://doi.org/10.1016/j.rse.2012.10.031

Patel, P., Srivastava, H.S., Panigrahy, S., Parihar, J.S., 2006. Comparative evaluation of the sensitivity of multi-polarized multi-frequency SAR backscatter to plant density. Int. J. Remote Sens. 27, 293–305. https://doi.org/10.1080/01431160500214050

Pekel, J.-F., Cottam, A., Gorelick, N., Belward, A.S., 2016. High-resolution mapping of global surface water and its long-term changes. Nature 540, 418–422. https://doi.org/10.1038/nature20584

Pickens, A.H., Hansen, M.C., Hancher, M., Stehman, S.V., Tyukavina, A., Potapov, P., Marroquin, B., Sherani, Z., 2020. Mapping and sampling to characterize global inland water dynamics from 1999 to 2018 with full Landsat time-series. Remote Sens. Environ. 243, 111792. https://doi.org/10.1016/j.rse.2020.111792

Pilliod, D.S., McCaffery, R.M., Arkle, R.S., Scherer, R.D., Cupples, J.B., Eby, L.A., Hossack, B.R., Lingo, H., Lohr, K.N., Maxell, B.A., McGuire, M.J., Mellison, C., Meyer, M.K., Munger, J.C., Slatauski, T., Van Horne, R., 2022. Importance of local weather and environmental gradients on demography of a broadly distributed temperate frog. Ecol. Indic. 136, 108648. https://doi.org/10.1016/j.ecolind.2022.108648

Poff, B., Koestner, K.A., Neary, D.G., Merritt, D., 2012. Threats to western United States riparian ecosystems: A bibliography (No. RMRS-GTR-269). U.S. Department of Agriculture, Forest Service, Rocky Mountain Research Station, Ft. Collins, CO. https://doi.org/10.2737/RMRS-GTR-269

Pollock, M.M., Beechie, T.J., Wheaton, J.M., Jordan, C.E., Bouwes, N., Weber, N., Volk, C., 2014. Using Beaver Dams to Restore Incised Stream Ecosystems. BioScience 64, 279–290. https://doi.org/10.1093/biosci/biu036

Prăvălie, R., 2016. Drylands extent and environmental issues. A global approach. Earth-Sci. Rev. 161, 259–278. https://doi.org/10.1016/j.earscirev.2016.08.003

Prober, S.M., Doerr, V.A.J., Broadhurst, L.M., Williams, K.J., Dickson, F., 2019. Shifting the conservation paradigm: a synthesis of options for renovating nature under climate change. Ecol. Monogr. 89, e01333. https://doi.org/10.1002/ecm.1333

Rayden, T., Jones, K.R., Austin, K., Radachowsky, J., 2023. Improving climate and biodiversity outcomes through restoration of forest integrity. Conserv. Biol. 37, e14163. https://doi.org/10.1111/cobi.14163

Reinhardt, J.R., Filippelli, S., Falkowski, M., Allred, B., Maestas, J.D., Carlson, J.C., Naugle, D.E., 2020. Quantifying Pinyon-Juniper Reduction within North America's Sagebrush Ecosystem. Rangel. Ecol. Manag. 73, 420–432. https://doi.org/10.1016/j.rama.2020.01.002

Rissman, A.R., Lozier, L., Comendant, T., Kareiva, P., Kiesecker, J.M., Shaw, M.R., Merenlender, A.M., 2007. Conservation Easements: Biodiversity Protection and Private Use. Conserv. Biol. 21, 709–718. https://doi.org/10.1111/j.1523-1739.2007.00660.x

Rockström, J., Gupta, J., Qin, D., Lade, S.J., Abrams, J.F., Andersen, L.S., Armstrong McKay, D.I., Bai, X., Bala, G., Bunn, S.E., Ciobanu, D., DeClerck, F., Ebi, K., Gifford, L., Gordon, C., Hasan, S., Kanie, N., Lenton, T.M., Loriani, S., Liverman, D.M., Mohamed, A.,

Nakicenovic, N., Obura, D., Ospina, D., Prodani, K., Rammelt, C., Sakschewski, B., Scholtens, J., Stewart-Koster, B., Tharammal, T., van Vuuren, D., Verburg, P.H., Winkelmann, R., Zimm, C., Bennett, E.M., Bringezu, S., Broadgate, W., Green, P.A., Huang, L., Jacobson, L., Ndehedehe, C., Pedde, S., Rocha, J., Scheffer, M., Schulte-Uebbing, L., de Vries, W., Xiao, C., Xu, C., Xu, X., Zafra-Calvo, N., Zhang, X., 2023. Safe and just Earth system boundaries. Nature 619, 102–111. https://doi.org/10.1038/s41586-023-06083-8

Shackelford, N., Dudney, J., Stueber, M.M., Temperton, V.M., Suding, K.L., 2024. Measuring at all scales: sourcing data for more flexible restoration references. Restor. Ecol. 32, e13541. https://doi.org/10.1111/rec.13541

Shrestha, N., Kolarik, N.E., Brandt, J.S., 2024. Mesic vegetation persistence: A new approach for monitoring spatial and temporal changes in water availability in dryland regions using cloud computing and the sentinel and Landsat constellations. Sci. Total Environ. 917, 170491. https://doi.org/10.1016/j.scitotenv.2024.170491

Silverman, N.L., Allred, B.W., Donnelly, J.P., Chapman, T.B., Maestas, J.D., Wheaton, J.M., White, J., Naugle, D.E., 2019. Low-tech riparian and wet meadow restoration increases vegetation productivity and resilience across semiarid rangelands: low-tech restoration increases vegetation productivity. Restor. Ecol. 27, 269–278. https://doi.org/10.1111/rec.12869

Skidmore, P., Wheaton, J., 2022. Riverscapes as natural infrastructure: Meeting challenges of climate adaptation and ecosystem restoration. Anthropocene 38, 100334. https://doi.org/10.1016/j.ancene.2022.100334

Stehman, S.V., Foody, G.M., 2019. Key issues in rigorous accuracy assessment of land cover products. Remote Sens. Environ. 231, 111199. https://doi.org/10.1016/j.rse.2019.05.018

Theobald, D.M., Harrison-Atlas, D., Monahan, W.B., Albano, C.M., 2015. Ecologically-Relevant Maps of Landforms and Physiographic Diversity for Climate Adaptation Planning. PLOS ONE 10, e0143619. https://doi.org/10.1371/journal.pone.0143619

Uzun, S., Tanir, T., Coelho, G. de A., Souza de Lima, A. de, Cassalho, F., Ferreira, C.M., 2021. Changes in snowmelt runoff timing in the contiguous United States. Hydrol. Process. 35, e14430. https://doi.org/10.1002/hyp.14430

Vanderhoof, M.K., Nieuwlandt, P., Golden, H.E., Lane, C.R., Christensen, J.R., Keenan, W., Dolan, W., 2025. Relating surface water dynamics in wetlands and lakes to spatial variability in hydrologic signatures. Wetl. Ecol. Manag. 33, 53. https://doi.org/10.1007/s11273-025-10066-z

Western, A.W., Grayson, R.B., Blöschl, G., Willgoose, G.R., McMahon, T.A., 1999. Observed spatial organization of soil moisture and its relation to terrain indices. Water Resour. Res. 35, 797–810. https://doi.org/10.1029/1998WR900065

Wohl, E., 2021. Legacy effects of loss of beavers in the continental United States. Environ. Res. Lett. 16, 025010. https://doi.org/10.1088/1748-9326/abd34e

Wohl, E., Rathburn, S., Dunn, S., Iskin, E., Katz, A., Marshall, A., Means-Brous, M., Scamardo, J., Triantafillou, S., Uno, H., 2024. Geomorphic context in process-based river restoration. River Res. Appl. 40, 322–340. https://doi.org/10.1002/rra.4236

Wyborn, C., Datta, A., Montana, J., Ryan, M., Leith, P., Chaffin, B., Miller, C., van Kerkhoff, L., 2019. Co-Producing Sustainability: Reordering the Governance of Science, Policy, and Practice. Annu. Rev. Environ. Resour. 44, 319–346. https://doi.org/10.1146/annurev-environ-101718-033103

Zupanc, A., 2020. Improving Cloud Detection with Machine Learning. Sentin. Hub Blog. URL https://medium.com/sentinel-hub/improving-cloud-detection-with-machine-learning-c09dc5d7cf13 (accessed 1.4.22).

Appendix

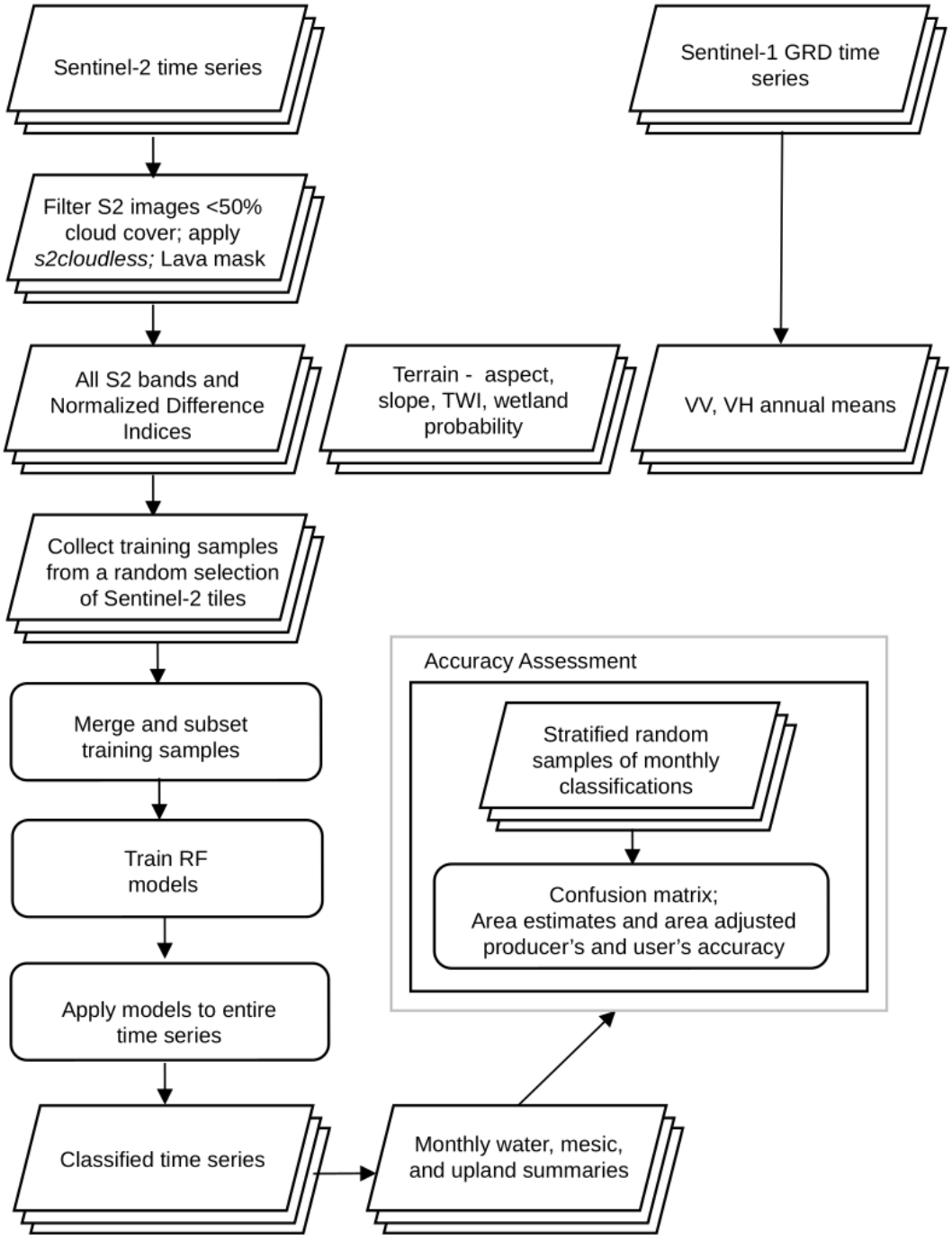

Figure S1. Workflow diagram for the time series classification and accuracy assessment.

Table S1. Confusion matrix June 2018.

			Ref	
		Upland	Mesic	Water
	Upland	134	1	1
Map	Mesic	7	66	0
	Water	1	0	90

Table S2. Confusion matrix July 2018.

			Ref	
		Upland	Mesic	Water
	Upland	150	1	0
Map	Mesic	7	58	0
	Water	0	0	84

Table S3. Confusion matrix August 2018.

			Ref	
		Upland	Mesic	Water
	Upland	164	1	1
Map	Mesic	4	49	0
	Water	1	0	80

Table S4. Confusion matrix September 2018.

			Ref	
		Upland	Mesic	Water
	Upland	178	2	2
Map	Mesic	2	41	0
	Water	1	0	74

Table S5. Confusion matrix June 2021.

			Ref	
		Upland	Mesic	Water
	Upland	129	3	1
Map	Mesic	8	76	0
	Water	1	0	82

Table S6. Confusion matrix July 2021.

		Ref		
		Upland	Mesic	Water
	Upland	140	2	3
Map	Mesic	9	71	0
	Water	1	0	74

Table S7. Confusion matrix August 2021.

			Ref	
		Upland	Mesic	Water
	Upland	163	3	1
Map	Mesic	8	48	0
	Water	3	0	74

Table S8. Confusion matrix September 2021.

			Ref	
		Upland	Mesic	Water
	Upland	173	3	0
Map	Mesic	6	40	0
	Water	3	0	75

Table S9. Confusion matrix June 2024.

			Ref	
		Upland	Mesic	Water
	Upland	128	0	0
Map	Mesic	22	60	0
	Water	2	0	88

Table S10. Confusion matrix July 2024.

			Ref	
		Upland	Mesic	Water
	Upland	137	0	0
Map	Mesic	21	56	0
	Water	2	0	84

Table S11. Confusion matrix August 2024.

			Ref	
		Upland	Mesic	Water
	Upland	165	0	0
Map	Mesic	13	38	0
	Water	3	1	80

Table S12. Confusion matrix September 2024.

			Ref	
		Upland	Mesic	Water
	Upland	185	1	1
Map	Mesic	9	26	0
	Water	6	0	72

Table S13. Counts of HUC12 units analyzed for each EPA level III ecoregion, % agriculture (crops/pasture), % federal land, % USFS, % BLM.

Ecoregion	**% Agriculture**	**% Federal**	**% USFS**	**% BLM**
Cascades	0.46	26.95	20.6	3.55
Eastern Cascades Slopes and Foothills	5.52	17.62	6.24	11.26
Blue Mountains	2.99	43.33	14.86	28.55
Middle Rockies	3.37	54.31	34.34	15.1
Sierra Nevada	0.06	44.35	28.34	4.51
Wasatch and Uinta Mountains	1.76	47.15	36.06	10.97
Southern Rockies	0.76	39.84	24.57	14.42
Idaho Batholith	0.29	71.41	65.64	6.86
Northwestern Glaciated Plains	45.06	10.43	1.00E-02	10.14
Northwestern Great Plains	14.31	29.22	0.51	27.34
High Plains	43.84	1.35	0.05	1.28
Columbia Plateau	40.31	6.86	0.35	4.96
Northern Basin and Range	3.45	80.82	2.92	76.44
Wyoming Basin	3.23	80.33	0.59	79.99
Central Basin and Range	2.37	78.92	6.04	72.77
Colorado Plateaus	2.95	68.46	1.84	66.01
Arizona/New Mexico Plateau	1.62	30.46	0.58	27.47
Snake River Plain	28.46	51.79	0.02	51.77
Mojave Basin and Range	0.26	66.76	1.2	46.62
Arizona/New Mexico Mountains	0.01	28.03	16.66	10.75

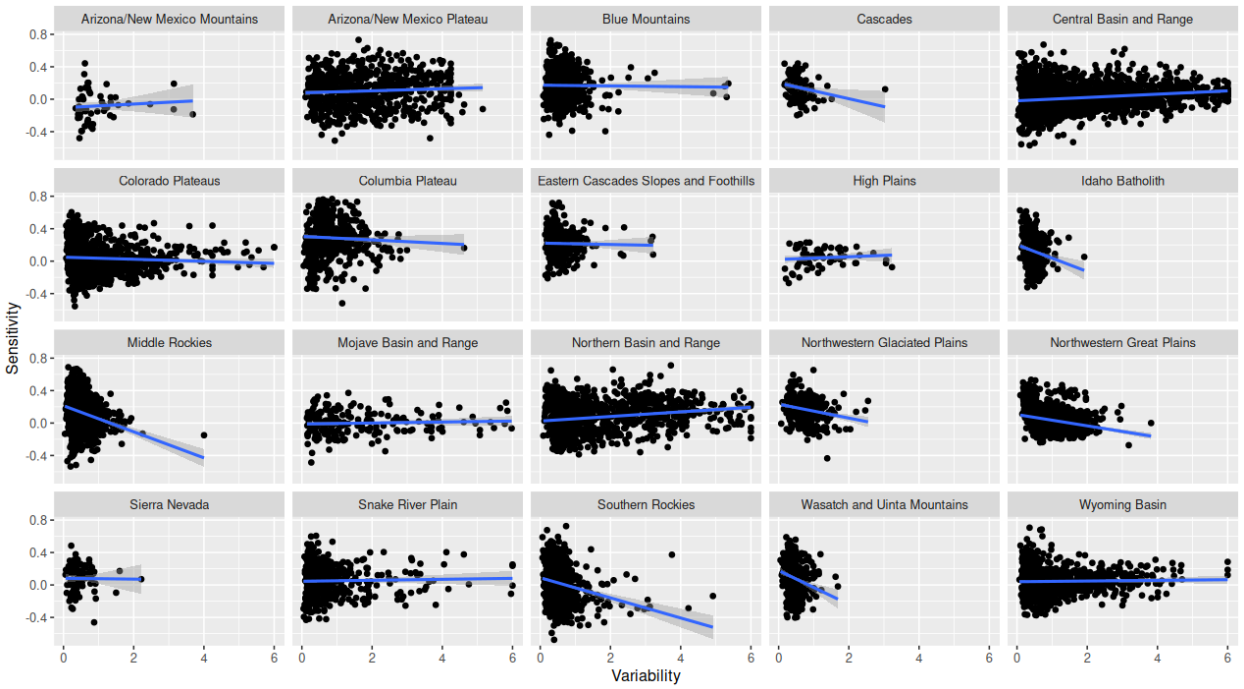

Figure S2. Plots of sensitivity (y-axis) and variability (x-axis of each HUC12 for each ecoregion in the sagebrush biome. Blue lines are fitted linear regressions to show general relationships between the two indicators.

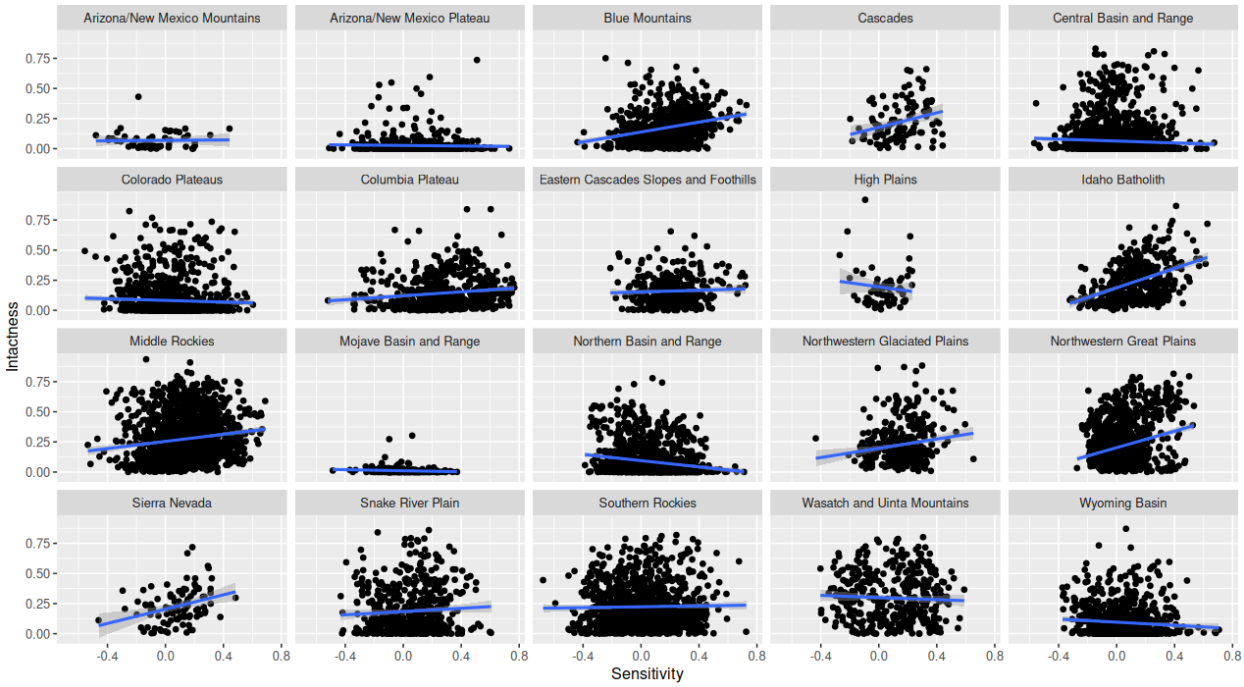

Figure S3. Plots of intactness (y-axis) and sensitivity (x-axs) of each HUC12 for each ecoregion in the sagebrush biome. Blue lines are fitted linear regressions to show general relationships between the two indicators.